University of Alberta
Printing Department

THE UNIVERSITY OF ALBERTA

A QUADRUPOLE LENS ION SOURCE FOR MASS SPECTROMETERS

by

Laurel E. Goodrich

A THESIS

SUBMITTED TO THE FACULTY OF GRADUATE STUDIES

IN PARTIAL FULFILLMENT OF THE REQUIREMENTS FOR THE DEGREE

OF MASTER OF SCIENCE

DEPARTMENT OF PHYSICS

Edmonton, Alberta

September, 1963

TABLE OF CONTENTS

LIST OF ILLUSTRATIONS

ACKNOWLEDGEMENT

The author gratefully acknowledges the assistance of Dr. G. L. Cumming who suggested and supervised the project, and of Dr. H. R. Krouse for his many valuable suggestions.

Thanks are also due to Mr. H. McCullough for his technical assistance and to Miss H. Hufnagel who typed the manuscript.

ABSTRACT

A mass spectrometer ion source employing a quadrupole lens pair in place of the conventional aperture lens arrangement has been constructed.

An initially parallel beam produced by a stack of equipotential rings was used as input to a quadrupole lens pair. The latter produces a wedge-shaped beam as required for maximum transmission through the beam tube of a mass spectrometer.

Complete design information has been calculated. The data are presented graphically.

The device was tested using a flourescent screen. Line focusses approximately .010" wide were obtained. The residual width seemed to be due partly to abberations in the ion chamber-focussing section and partly to the grid used to terminate the uniform field accelerating section.

The quadrupole source gave an improvement in sensitivity by a factor of about 3 over the conventional source.

I. INTRODUCTION

A wide variety of ion sources have been employed in mass spectrometric studies. Amongst the principal types may be included devices which produce ions by electron impact, surface ionization, spark and arc discharge, high-field emission and photo-ionization. However, for isotopic ratio studies only two principal types are widely used. These are, namely, the electron-impact source and the surface ionization source.

In the electron-impact source, originally devised by Dempster but brought to its present form by Nier, the material to be studied is introduced, in the form of a gas, into the ionization chamber where it is ionized by collision with an electron beam moving parallel to the exit slit of the ionization chamber. The ions are withdrawn from the ionization chamber, accelerated and collimated to a line focus at the exit of the source by using a suitable arrangement of electrodes and collimating slits. The ions emerging from the exit slit of the source pass into the magnetic field of the mass spectrometer where they are analyzed according to their mass.

The principal features of the electron-impact source may be summarized as follows. The ions arising from an electron-impact source are nearly homogeneous in energy,

energy spreads of $\sim$ 0.05 eV being typical. This represents a considerable advantage when such a source is to be used with a direction - focussing* mass spectrometer, as is the usual case. The ionization efficiency of the electron impact source depends upon the geometry of the ionization chamber as well as upon the ionization cross-section of the atom involved. Typical efficiencies are of the order 10^{-4}%. Owing to the large transmission losses in the conventional electrode arrangement (see below) generally only about 1% of the ions formed in the source are actually collected. Typical sensitivities** are of the order 10^{-10} amps ion current for a total flow of 2×10^{-3} litres/second at 1 μ pressure. The actual sensitivity obtained in any particular case will, of course, depend upon the species of atom (or molecule) involved. Only very small amounts of material are required

---

* Direction - focussing mass spectrometers are instruments capable of refocussing (first order approximation) an ion beam diverging at a small angle from the object point, provided the ion beam is homogeneous in energy. The velocity dependence of the focussing properties may be removed by using combinations of electric and magnetic fields. Such systems are termed double-focussing.

** By sensitivity is meant the number of ions ultimately extracted from the source per unit number of atoms introduced into the ionization chamber. It is thus the product of the ionization efficiency and a constant factor to take account of transmission losses in the source.

for an analysis. The following data, taken from the literature, will serve to indicate the situation:

In the case of xenon, 2×10^{-9} cc (5×10^{10} atoms) of a single isotope is sufficient for an analysis[16] while 5×10^{5} atoms of any xenon isotope can be detected using suitable operating techniques.[19] These figures assume conventional detection apparatus. Using an electron-multipier in place of the normal collector arrangement it is even possible to detect individual ions.

Although the electron-impact source is best suited to the analysis of materials which exist under normal conditions as a gas or which possess an appreciable vapour pressure, non-volatile solids may be handled by using a furnace or oven located in the vicinity of the ionization chamber.

However, for the analysis of a number of important elements, notably the rare earths as well as Sc, Ga, Y, In, Cs, La, Ce, Rb, Sr, and Tl,[15] the electron impact source is less efficient than other types. For such materials the surface ionization source is commonly used.

Positive ions emitted from a salt coated on a hot filament were first observed by Gehrcke and Reichenheim in 1906. Somewhat later (1918) the phenomenon was applied by Dempster to mass spectroscopy. Kunsman (1925) did important pioneer work relevant to the mechanism of this positive-ion emission and the methods of catalyzing it.

In the surface ionization source a salt of the element to be studied is coated on a filament which is then heated in vacuum. If the filament has a higher affinity for electrons than the material applied to it, a fraction N_+/N_o of the material evaporated will be positively ionized. The efficiency of the process, including the reemission as ions of neutral atoms striking the hot filament has been shown theoretically[18] to obey the exponential relation

$$N_+/N_o = \exp\left[\frac{e(w-\varphi)}{kT}\right]$$

where w = work function of the filament

φ = ionization potential of the evaporated atom

T = temperature of the filament.

In practice the actual yield of positive ions depends to a very marked degree upon the chemical compound used. For example, Inghram and Hayden[15] give the following data on Caesium salts:

> Using 10 $\mu g/mm^2$ of CsCl deposited on a tungsten filament, the ratio N_+/N_o for Cs^+ ions is approximately 10^{-4}. Using 10 $\mu g/mm^2$ of Cs_2SO_4 also deposited on tungsten the ratio N_+/N_o for Cs^+ ions is approximately 1.

The gross difference in emission in the two cases may be explained by the fact that most of the CsCl evaporates before the ionization temperature is reached. Such difficulties

have been overcome by certain workers, notably Inghram and Chupka[14] who have used a two-filament arrangement in which the volatile salt is evaporated at a relatively low temperature from one filament, the vapour being ionized when it impinges on an adjacent filament maintained at a much higher temperature.

Surface ionization sources produce ions which are practically monoenergetic. Energy spreads of approximately 0.2 eV are typical and, although this figure is larger than that for the electron impact source, nevertheless it is small enough that completely satisfactory results may be obtained with single focussing instruments.

Only extremely minute amounts of material are required for an analysis using surface ionization sources. For example Hess et al.[13] using isotope dilution techniques* and a conventional collector system have detected 2×10^{-13} gm (5×10^{8} atoms) of Uranium with a precision of 1 - 2 percent. Using an electron-multiplier considerably smaller amounts may be detected.

---

* Isotope Dilution is a sensitive method for determining the amount of an element present in a sample. The quantity of an element is estimated from the change produced in its isotopic composition by the addition of a known quantity of a stable isotopic tracer of that element.

The most serious disadvantage of the surface ionization source is the isotopic fractionation which inevitably occurs during evaporation of the material from the filament. If the process is one of free evaporation from a liquid, which is often the case, the isotopes evaporate at rates which are inversely proportional to the square roots of their masses and the appropriate correction factor can be applied to the data. This is, of course, important only for absolute ratio determinations.

From the ion-optical point of view, surface ionization sources are essentially similar to electron impact sources. The following schematic illustrates the conventional electrode arrangement and is the one currently used in this laboratory.

Fig. I

Conventional Ion Source

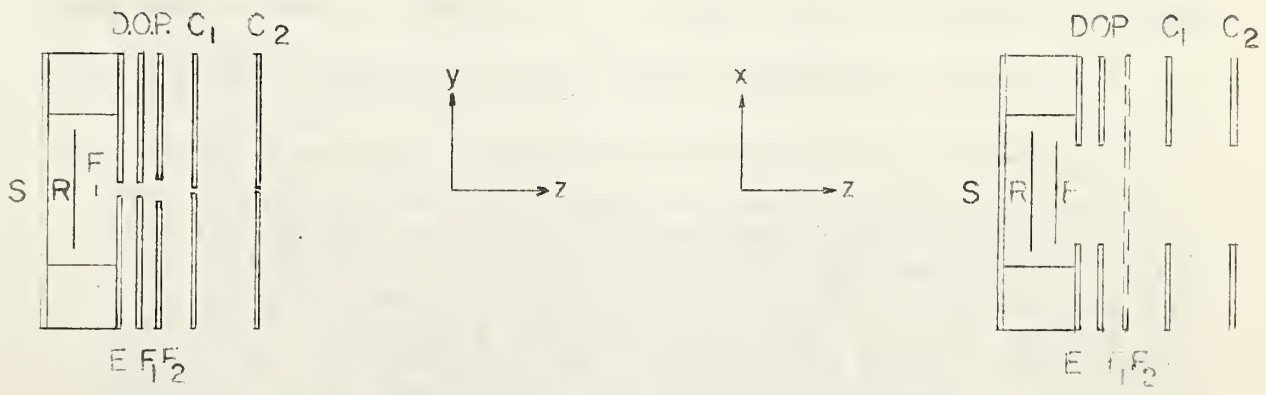

S is a shield or case which together with the exit plate E comprises the ionization chamber.

R is a repeller plate which is used to urge ions emitted from the filament F out through the exit slit in plate E.

D.O.P. (Drawing out Plate) is held at a potential slightly ($\sim$ 100 v) below that of the filament and thus serves to draw ions out of the ionization chamber and into the region of the electrode F_1F_2.

F_1 and F_2, which are half-plates insulated electrically from one another, together comprise the focussing electrode. By holding F_1 and F_2 at slightly different potentials a useful control over the lateral position of the ion beam is obtained. The majority of the acceleration through the ion source takes place between the focus plate and C_1.

In the conventional arrangement, the apertures in all plates are long narrow slits. Thus the three electrodes E, D.O.P, and F_1F_2 each act as slit-aperture ion lenses* the combined effect of which is to focus the ion beam to a cross-over in the vicinity of the final collimator slit C_2.

---

* The theory of the slit aperture lens has been given by Harnwell[12] who obtains an approximate expression for the focal length: $f = 2v/(E_2-E_1)$, where E_2 and E_1 are field strengths at the exit and entrance sides respectively of the plane containing the aperture and v is the energy of an ion at the position of the aperture plate. The expression is valid assuming slit widths much smaller than the separation between electrodes and assuming small penetration of the fields.

From the point of view of obtaining maximum transmission through the source, of those ions formed at the filament, the conventional design has several disadvantages.

To achieve significant focussing effects with reasonable field strengths the width of the apertures in the focussing electrodes must be small and, in consequence, a considerable proportion of the beam may be obstructed. From observation of the deposits left on the electrodes after several hours operation using a filament heavily loaded with Cs_2SO_4, it appears, that of those ions formed, approximately 1/2 to 2/3 are obstructed by the exit plate of the ionization chamber. Further losses occur at the D.O.P.

Since the slit lens arrangement is incapable of providing a well defined crossover of small angular divergence as is required to obtain significant resolution* in the mass spectrometer, grounded collimator slits C_1 and C_2 having apertures much narrower than the width of the beam are used, resulting in further transmission losses.

---

* Resolution is a measure of the ability of a mass spectrometer to separate ion beams according to their mass. Two ion beams of different mass are said to be just resolved when the distance between their centres equals the beam width at the image point of the mass spectrometer. For the conventional direction-focussing sector magnetic analyzer used symmetrically (ie. object and image distance equal), the resolution is given, in a first approximation, by the relation: $R = M/\Delta M = r/(S_s+S_c)$, where r is the radius of curvature of the ion trajectory in the magnetic field and S_s and S_c are the widths of the source and collector slits respectively. In practice a number of abberations exist the most important of which is spherical abberation. To take account of this, a term $\theta^2 r$ must be added where θ is the half-angular divergence of the beam beyond the source slit. These matters are discussed in detail by Barnard[1].

In the conventional source no provision is made for focussing the beam in the x-z (slit long-axis) plane. The consequent transmission losses can be considerable since not only is the beam obstructed by the source electrodes, but also a sizable fraction of it may not actually reach the Faraday cage of the collector since the latter is located some distance ($\sim$ 2 to 3 ft.) away. Overall transmission losses in the conventional source may amount to as much as approximately 99%.[1]

One further point in connection with the use of slit aperture lenses in the conventional source needs be made. Whenever electrodes are bombarded by a sufficiently energetic ion beam, two effects, both undesirable in an ion source, may occur. These are, namely, secondary electron emission and polarization. Furthermore, the conditions under which secondary electron emission effects are minimized are precisely the ones under which polarization effects are maximized.* In order to avoid spurious effects deriving from these two causes it is clearly desirable that the ion beam pass through the source with minimal obstruction by the electrode surfaces. This condition can not be met using aperture lenses.

---

* Secondary emission yields are greatest for ions incident normally upon a smooth metal surface. Polarization is greatest for ions incident at grazing angles upon a rough or porous metal surface.

Following the work of Giese[10] and Kinzer and Carr[17], an ion source has been constructed which attempts to overcome some of the difficulties inherent in the conventional arrangement.

In place of the usual focussing and collimating slits, the new source employs a quadrupole lens pair to focus an initially parallel ion beam of rectangular cross-section to a line focus at the object point of the mass spectrometer. Such an arrangement might be expected to provide increased sensitivity over that obtained in the conventional source since no narrow apertures exist to obstruct the beam and also because control is gained over focussing conditions in the x-z plane. In addition, some improvement in resolution seems not out of the question. A very narrow line focus ought to be possible provided abberations other than within the quadrupole lens can be minimized. The quadrupole lens itself is relatively free from spherical abberation.

II. THEORY OF THE QUADRUPOLE LENS

A. The Trajectory Equations

Quadrupole lenses for a variety of purposes have been constructed using both magnetic and electrostatic fields.[2,3;9,10;20-23] However, for applications in mass spectrometry, magnetic lenses are undesirable and hence only the electrostatic case will be considered here.

For a charged particle moving in the z direction through a field of the form:

$$\vec{E} = k(x\hat{i} - y\hat{j})^{*}$$

the equations of motion are:

$$\ddot{x} = \frac{e}{m} kx$$

$$\ddot{y} = -\frac{e}{m} ky$$

$$\ddot{z} = 0$$

---

* 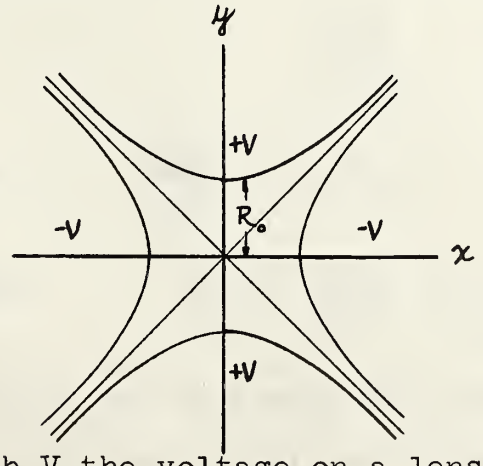

The equipotentials of such a field are given by the family of curves:

$$\Phi = \int \vec{E} \cdot d\vec{\ell} = \frac{k}{2}(y^2 - x^2) = \text{constant}$$

which are hyperbolas with asymptotes $y = \pm x$. Hence we conclude the pole pieces should by hyperbolas asymptotic to the lines $y = \pm x$, as shown in the figure (these matters are discussed further in Appendix 1). With V the voltage on a lens element and $2R_o$ the aperture, $k = 2V/R_o^2$.

Assuming that the trajectories in the x - z and y - z planes make only small angles with the z axis (in the paraxial approximation), the magnitude of the particle's velocity

$$|\vec{v}| = v = \frac{dz}{dt}\left[1 + \left(\frac{dx}{dz}\right)^2 + \left(\frac{dy}{dz}\right)^2\right]^{1/2}$$

is given approximately by

$$v \approx \frac{dz}{dt} ,$$

which is a constant. Also, since

$$\frac{dx}{dt} \approx \frac{dx}{dz}\frac{dz}{dt} \approx \frac{dx}{dz} v$$

$$\frac{d^2x}{dt^2} \approx \frac{v^2 d^2x}{dz^2} .$$

Similarly, $$\frac{d^2y}{dt^2} \approx \frac{v^2 d^2y}{dz^2}$$

Thus the equations of the trajectories become:

$$\frac{d^2x}{dz^2} = \omega^2 x \qquad \text{for the divergent plane}$$

and $$\frac{d^2y}{dz^2} = -\omega^2 y \qquad \text{for the convergent plane,}$$

where $$\omega^2 = \frac{ek}{mv^2} = \frac{V}{R_o^2 E}$$

where E is the energy in volts of the incident particle and V and R_o are as defined above.

The following definitions are taken as boundary conditions:

$$x(0) = x_o \qquad x(d) = x_1$$

$$\partial x/\partial z \,|_{z=o} = \dot{x}_o \qquad \partial x/\partial z \,|_{z=d} = \dot{x}_1$$

where the field is assumed to extend over a region of length d*. Similar definitions apply to the y-z plane.

Trajectories Through a Quadrupole Lens

Fig. II

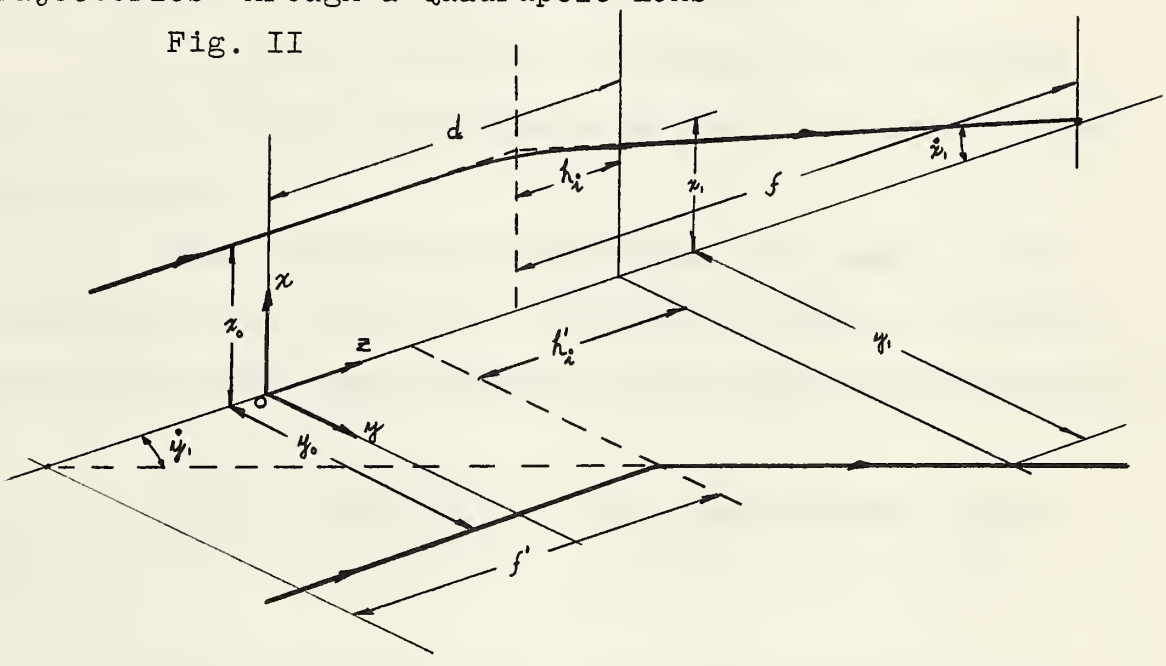

Inserting the boundary conditons, the trajectory equation in the divergent plane becomes:

$$x_1 = x_o \cosh \omega d + \frac{\dot{x}_o}{\omega} \sinh \omega d$$

---

* See Appendix I

Also $$\dot{x}_1 = x_o \omega \sinh \omega d + \dot{x}_o \cosh \omega d$$

Similarly, equations for the trajectory in the convergent plane can be written:

$$y_1 = y_o \cos \omega d + \frac{\dot{y}_o}{\omega} \sin \omega d$$

$$\dot{y}_1 = -y_o \omega \sin \omega d + \dot{y}_o \cos \omega d$$

B. A Matrix Formulation for the Quadrupole Lens

It is most convenient to express the trajectory equation in a matrix formalism as is done in ordinary geometrical optics.

Then the off-axis displacement and angle of the trajectory at the lens exit are given in terms of similar quantities at the lens entrance by the matrix transformations

$$\begin{pmatrix} x_1 \\ \dot{x}_1 \end{pmatrix} = (D) \begin{pmatrix} x_o \\ \dot{x}_o \end{pmatrix} \qquad \text{for the divergent plane}$$

and $$\begin{pmatrix} y_1 \\ \dot{y}_1 \end{pmatrix} = (C) \begin{pmatrix} y_o \\ \dot{y}_o \end{pmatrix} \qquad \text{for the convergent plane.}$$

The divergence and convergence matrices are given respectively by

$$(D) = \begin{pmatrix} \cosh \omega d & \frac{1}{\omega} \sinh \omega d \\ -\omega \sinh \omega d & \cosh \omega d \end{pmatrix} \qquad (1)$$

$$(C) = \begin{pmatrix} \cos \omega d & \frac{1}{\omega} \sin \omega d \\ -\omega \sin \omega d & \cos \omega d \end{pmatrix} . \qquad (2)$$

Using the matrix method* it is a simple matter to show that the convergence matrix (C) focusses an incident parallel beam on to the z axis.

Let z_1 be the distance, measured with respect to the lens exit, at which the beam crosses the z axis. The transformation consists of a lens (C) followed by a drift space of length z_1, whilst the boundary conditions are

$$\dot{x}_o = 0, \qquad x_1 = 0$$

(It should be noted that a more general definition for x_o, x_1, etc. than that previously used has been assumed; viz. the relevant quantities are considered to be evaluated at the entrance and exit to the entire system). Thus the transformation is described by

$$\begin{pmatrix} 0 \\ \dot{x}_1 \end{pmatrix} = \begin{pmatrix} 1 & z_1 \\ 0 & 1 \end{pmatrix} (C) \begin{pmatrix} x_o \\ 0 \end{pmatrix}$$

Inserting equation (2) gives

$$z_1 = \frac{1}{\omega \tan \omega d} .$$

z_1 is not a focal length in the usual sense since it is measured from the lens exit and not from the exit principal plane.

---

* See Appendix II

Expressions for the focal length and positions of the principal planes may be found using the relation*:

$$(C) = \begin{bmatrix} 1 - h_i/f & h_o+h_i - \frac{h_o h_i}{f} \\ -1/f & 1 - h_o/f \end{bmatrix} \qquad (3)$$

which is valid if the quadrupole can be represented by a thick lens.

The exit principal plane is located at a distance h_o before the lens exit whilst the entrance principal plane is located at a distance h_i after the lens entrance.

Equating elements in (3) we find, for the converging plane

$$1/f = \omega \sin \omega d$$

and $$h_o = h_i = (1 - \cos \omega d)/\omega \sin \omega d$$

By inserting (D) in equation (3) we find for the diverging plane:

$$1/f' = -\omega \sinh \omega d$$

$$h_o' = h_i' = (\cosh \omega d - 1)/\omega \sinh \omega d$$

By definition, a lens is thin if its two principal planes coincide. Thus for the quadrupole lens, the criterion that it be thin is

$$h_o = h_i = d/2 \ .$$

---

* See Appendix II

Expanding the expressions for the positions of the principal planes in powers of ωd, we obtain:

$$h_o = h_i = \frac{d}{2}\left(1+\frac{(\omega d)^2}{12} + \ldots.\right)$$ for the converging plane, and

$$h_o' = h_i' = \frac{d}{2}\left(1 - \frac{(\omega d)^2}{12}\right)$$

for the diverging plane. Thus the quadrupole behaves as a thin lens if

$$(\omega d)^2 \ll 1.$$

In this approximation also the expansions

$$1/f = \omega^2 d\left(1 - \frac{(\omega d)^2}{6} + \ldots\right)$$

$$1/f' = -\omega^2 d\left(1 + \frac{\omega^2 d^2}{6} + \ldots\right)$$

yield $$1/f = -1/f' \approx \omega^2 d \ .$$

Since, individually, quadrupole lenses are convergent in one plane but divergent in the other, it is necessary, in order to obtain a system which is convergent in both planes, to combine two or more quadrupoles with the convergence plane of the second lens rotated 90^o with respect to that of the first. Thus, for a system of two quadrupoles, the lens will be first convergent then divergent in one plane (the C. D. plane) while in the other plane (D. C. plane) it will be

first divergent, then convergent.

Assuming two quadrupoles, both of length d, separated a distance L between pole pieces, the transformation becomes in the C. D. plane:

$$(M) = \begin{pmatrix} \cosh \omega_2 & \frac{1}{\omega_2} \sinh \omega_2 \\ \omega_2 \sinh \omega_2 & \cosh \omega_2 \end{pmatrix} \quad \begin{pmatrix} 1 & L \\ 0 & 1 \end{pmatrix} \quad \begin{pmatrix} \cos \omega_1 & \frac{1}{\omega_1} \sin \omega_1 \\ -\omega_1 \sin \omega_1 & \cos \omega_1 \end{pmatrix}$$

and in the D. C. plane:

$$(N) = \begin{pmatrix} \cos \omega_2 & \frac{1}{\omega_2} \sin \omega_2 \\ -\omega_2 \sin \omega_2 & \cos \omega_2 \end{pmatrix} \quad \begin{pmatrix} 1 & L \\ 0 & 1 \end{pmatrix} \quad \begin{pmatrix} \cosh \omega_1 & \frac{1}{\omega_1} \sinh \omega_1 \\ \omega_1 \sinh \omega_1 & \cosh \omega_1 \end{pmatrix}$$

where for convenience d has been chosen as the unit of length.

Carrying out the multiplication we find for the matrix elements:

$$M_{11} = \cosh \omega_2 \cos \omega_1 - L\omega_1 \cosh \omega_2 \sin \omega_1 - \frac{\omega_1}{\omega_2} \sinh \omega_2 \sin \omega_1$$

$$M_{12} = \frac{1}{\omega_1} \cosh \omega_2 \sin \omega_1 + L \cosh \omega_2 \cos \omega_1 + \frac{1}{\omega_2} \sinh \omega_2 \cos \omega_1$$

$$M_{21} = \omega_2 \sinh \omega_2 \cos \omega_1 - L\omega_1\omega_2 \sinh \omega_2 \sin \omega_1 - \omega_1 \cosh \omega_2 \sin \omega_1$$

$$M_{22} = \frac{\omega_2}{\omega_1} \sinh \omega_2 \sin \omega_1 + L\omega_2 \sinh \omega_2 \cos \omega_1 + \cosh \omega_2 \cos \omega_1$$

(C. D. Plane)

and

$$N_{11} = \cos \omega_2 \cosh \omega_1 + L\omega_1 \cos \omega_2 \sinh \omega_1 + \frac{\omega_1}{\omega_2} \sin \omega_2 \sinh \omega_1$$

$$N_{12} = \frac{1}{\omega_1}\cos \omega_2 \sinh \omega_1 + L \cos \omega_2 \cosh \omega_1 + \frac{1}{\omega_2} \sin \omega_2 \cosh \omega_1$$

$$N_{21} = \omega_1 \cos \omega_2 \sinh \omega_1 - L\omega_1\omega_2 \sin \omega_2 \sinh \omega_1 - \omega_2 \sin \omega_2 \cosh \omega_1$$

$$N_{22} = \cos \omega_2 \cosh \omega_1 - L\omega_2 \sin \omega_2 \cosh \omega_1 - \frac{\omega_2}{\omega_1} \sin \omega_2 \sinh \omega_1$$

(D. C. plane)

By inspection, the following relations are seen to hold:

$$M_{11}(\omega_1,\omega_2) = N_{22}(\omega_2,\omega_1)$$

$$M_{12}(\omega_1,\omega_2) = N_{12}(\omega_2,\omega_1)$$

$$M_{21}(\omega_1,\omega_2) = N_{21}(\omega_2,\omega_1)$$

$$M_{22}(\omega_1,\omega_2) = N_{11}(\omega_2,\omega_1)$$

Since furthermore the transformation matrices are orthogonal:

$$M_{11}M_{22} - M_{12}M_{21} = N_{11}N_{22} - N_{12}N_{21} = 1$$

Thus the eight expressions for the matrix elements are reduced to three independant relations which, in principle, could be solved for the three lens parameters ω_1, ω_2 and L. However, since this is analytically impossible it is necessary to resort to a graphical method.

In the literature, graphical methods are treated by at least two authors. Rosenblatt[20] provides curves of

$$h_o(\omega,\gamma) = h_i'(\omega,1/\gamma)$$

$$h_i(\omega,\gamma) = h_o'(\omega,1/\gamma)$$

$$f(\omega,\gamma) = f'(\omega,1/\gamma)$$

where $\omega = (\omega_1\omega_2)^{1/2}$ is the mean lens "strength"

and $\gamma = (\omega_1/\omega_2)^{1/2}$ is the asymmetry parameter.

Given object and image distances S_o, S_o' and S_i, S_i' in the C. D. and D. C. planes respectively, the curves may be used to find appropriate values of ω and γ by trial and error.

Enge's[8] method differs from this. Using the fact that the tangent to the hyperbolic curve at the exit of the first lens must intercept the optic axis at the same point as the tangent to the trigonometric curve from the entrance of the second lens (D. C. plane), a relation which must be satisfied by ω_1 and ω_2 is obtained. A second relation may be obtained by considering conditions in the C. D. plane.

Curves of the position of the intercept x_c are plotted versus ωd with object and image distances in both planes taken as parameters. From the curves, the appropriate values of $\omega_1 d$, $\omega_2 d$ may be found. Finally, curves of image distance versus $(\omega_1 d)^2$ and versus $(\omega_2 d)^2$ with object distance as parameters are given. These refer only to the case of

stigmatic objects and images.

For the present application however, it is required to focus a beam incident parallel to the axis such that in one plane the crossover occurs relatively close to the lens, while in a perpendicular plane the beam remains parallel or is slightly convergent, as the following sketch will make clear.

Trajectories Through a Quadrupole Lens Pair

Fig. III

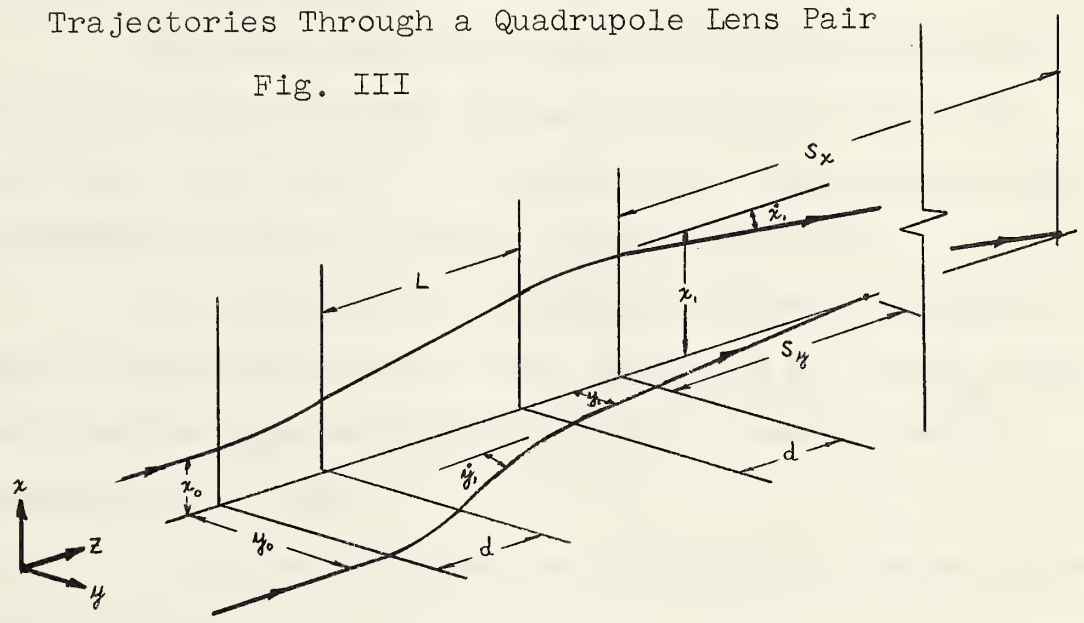

Since data relevant to this particular situation were not available it was necessary to carry out calculations. The cumbersome complexities of graphical computation were avoided by using a digital computer.

Referring to the diagram above, it should be noted that the following choice of coordinates has been made (this convention is adhered to in all succeeding work). The z axis lies along the direction of motion of the ion beam. The x axis is chosen to lie in the plane of the analyzer magnetic field, ie. parallel to the long axis of the defining slit in a conventional ion source. Then the near-focussing plane is the y-z plane.

The above drawing illustrates beam trajectories in both planes with the lens system oriented such that the near-focus plane is a C. D. combination. This orientation is assumed in the calculations immediately below.

For the case of a stigmatic object at infinity, simple expressions for the image distances S_y, and S_x measured from the lens exit may be found in terms of matrix elements for the lens.

Since in this case the lens relation becomes, for the y - z plane

$$Pi_y = F_y$$

where Pi_y is the image distance measured from the exit principal plane, and, referring to Appendix II,

$$Pi_y = Si_y + \frac{M_{11}-1}{M_{21}}$$

while

$$F_y = -1/M_{21}$$

we find

$$S_y = -M_{11}/M_{21} \quad ,$$

in units of d, the length of the lens element. Similarly,

$$S_x = -N_{11}/N_{21} \quad .$$

It is required to find solutions ω_1, ω_2, which are simultaneously solutions of the above equations. In order to formulate the problem in a form amenable to digital computation, Newton's method was used.

Define two new functions:

$$f(x,y,L) = S_x + \frac{N_{11}(x,y,L)}{N_{21}(x,y,L)}$$

$$g(x,y,L) = S_y + \frac{M_{11}(x,y,L)}{M_{21}(x,y,L)}$$

treating L, S_x, S_y as parameters solutions x, y are sought such that

$$f(x,y,L) = g(x,y,L) = 0$$

Assume x_1, y_1 are values in the neighbourhood of the exact solution; x, y.

Expand f and g in Taylor series about x_1, y_1, retaining only first order terms:

$$0 = f(x,y) = f(x_1,y_1) + \left.\frac{\partial f}{\partial x}\right|_{x_1} h + \left.\frac{\partial f}{\partial y}\right|_{y_1} k + \ldots$$

$$0 = g(x,y) = g(x_1,y_1) + \left.\frac{\partial g}{\partial x}\right|_{x_1} h + \left.\frac{\partial g}{\partial y}\right|_{y_1} k + \ldots$$

$$\text{then} \qquad h = \frac{-f(x_1,y_1)\,\frac{\partial g}{\partial y_1} + g(x_1,y_1)\,\frac{\partial f}{\partial y_1}}{\frac{\partial f}{\partial x_1}\,\frac{\partial g}{\partial y_1} - \frac{\partial f}{\partial y_1}\,\frac{\partial g}{\partial x_1}}$$

$$k = \frac{-g(x_1,y_1)\,\frac{\partial f}{\partial x_1} + f(x_1,y_1)\,\frac{\partial g}{\partial x_1}}{\frac{\partial f}{\partial x_1}\,\frac{\partial g}{\partial y_1} - \frac{\partial f}{\partial y_1}\,\frac{\partial g}{\partial x_1}}$$

The procedure in using Newtons method is as follows. Given x_1, y_1 as initial starting values, h and k are calculated, as increments to be added to x_1, y_1 to give

$$x_2 = x_1 + h$$

$$y_2 = y_1 + k \quad .$$

The new values x_2, y_2 will be a closer approximation to the solution than were x_1, y_1. The procedure is repeated using x_2, y_2 to calculate new increments h_1, k_1 which added to x_2, y_2 give even closer approximations to the solution. The procedure is repeated to give any desired degree of accuracy.

A computer programme was set up along these lines. However some difficulty was had in choosing suitable initial values. This was finally surmounted by inserting loops in the programme which caused the initial value x to be incremented in the event that x became unreasonably large or negative. By unreasonably large is meant numbers greater than the capacity of the computer, ie. e^{38}. Of course, it is physically meaningless for x to be negative.

One unexpected result emerged. It was cursorily assumed that solutions should exist for all positive values of S_x and S_y. However, this proved not to be the case. For a given S_y, there is a maximum value which can be assumed by S_x, ie. the "astigmatism" of the system is limited. It was found that greater "astigmatism" is achieved if the focus plane is a C. D. combination.

A copy of the programme ultimately used is given below. In terms of our present notation the computer symbols used are:

$x = \omega_1$ $\qquad$ $y = \omega_2$

$SX = S_y$ $\qquad$ $SZ = S_x$

$BIGL = L$

$SM21 = M_{21}(\omega_1, \omega_2)$ $\qquad$ $BM21 = N_{21}(\omega_1, \omega_2)$

$SM11 = M_{11}(\omega_1, \omega_2)$ $\qquad$ $BM22 = N_{11}(\omega_1, \omega_2)$

```
..I 903185 QUADRUPOLE ION SOURCE
..LOAD FORGO CLOCK 20000 ALLOW
 1     READ2,OMEG,GAMM,EPSIL,BIGL,SX,SZ
 2     FORMAT(F6.3,F6.3,E10.5,F6.3,F8.2,F8.2)
 10    SAM = 0.0
       OMEG = 0.05
 9     X=OMEG*GAMM
       Y=OMEG/GAMM
       SMH=0.0
       SMK=0.0
 3     X=X+SMH
       Y=Y+SMK
       IF(X)500,500,555
 555   IF(X-38.0)400,500,500
 400   AA=EXPF(X)
       BB=EXPF(Y)
       AX=AA-1.0/AA
       BX=AA+1.0/AA
       AY=BB-1.0/BB
       BY=BB+1.0/BB
       T=COSF(X)
       S=SINF(X)
       R=COSF(Y)
       W=SINF(Y)
       BM21=(X*AX*R-(BIGL*X*AX+BX)*Y*W)/2.
       BM22=(X*AX*W/Y+(BX+BIGL*X*AX)*R)/2.
       F=-SZ-BM22/BM21
       C=(X*AX/Y**2+BIGL*X*AX+BX)*W-X*AX*R/Y
       O=X*AX*W+(BIGL*A*AX+BX)*(W+Y*R)
       A=(BM21*C-BM22*O)/(2.*BM21**2)
       CA=AX*(W/Y+R+BIGL*R)+BX*(W*X/Y+BIGL*X*R)
       OA=R*(AX+X*BX)=Y*W*(AX+BIGL*(AX+X*BX))
       B=-(BM21*CA-BM22*OA)/(2.*BM21**2)
       SM21=(Y*AY*T-BIGL*X*Y*AY*S-X*BY*S)/2.
       SM11=(BY*T-BIGL*X*BY*S-X*AY*S/Y)/2.
       G=-SX-SM11/SM21
       DB=BY*S+(AY/Y+BIGL*BY)*(S+X*T)
       OB=Y*AY*S+(BIGL*Y*AY+BY)*(S+X*T)
       P=(SM21*DB-SM11*OB)/(2.*SM21**2)
       DC=(T-BIGL*X*S)*AY-X*S*(BY/Y-AY/Y**2)
       OC=(T-BIGL*X*S)*(AY+Y*BY)-X*S*AY
       Q=-(SM21*DC-SM11*OC)/(2.*SM21**2)
       SMH=(Q*F-G*A)/(A*P-Q*B)
       SMK=(P*F-G*B)/(Q*B-P*A)
       DEV=ABSF(SMH)+ABSF(SMK)
       IF(DEV-EPSIL)4,4,3
 4     OMEG=SQRTF(X*Y)
       GAMM=SQRTF(X/Y)
       PUNCH303,X,Y,BIGL
 303   FORMAT(5H X = F6.3,5H Y = F6.3,8H BIGL = F6.3)
       PUNCH101,SX,SZ,OMEG,GAMM
```

```
 101  FORMAT(6H SX = F8.2,6H SZ = F8.2,8H OMEG = F5.3,8H
GAMM = F6.3)
      PUNCH202,SM21,BM21,SM11,BM22
 202  FORMAT(7HSM21 = F8.5,8H BM21 = F8,5.8H SM11 = F6.3,8H BM22
= F6.3)
      GO TO 1
 500  IF(SAM-10.0)600,700,700
 600  OMEG = OMEG+0.2
      SAM = SAM+1.0
      GO TO 9
 700  PUNCH 701
 701  FORMAT(13H NO SOLUTION.)
      GO TO 1
      END
```

As explained in the introduction it is important, in the present application, to know values of the half-angle of divergence of the beam beyond the cross-over in the y - z plane.

Assuming the y - z plane to be a C. D. plane, the matrix transformation for an initially parallel beam is described by:

$$\begin{pmatrix} y_1 \\ \dot{y}_1 \end{pmatrix} = \begin{pmatrix} M_{11} & M_{12} \\ M_{21} & M_{22} \end{pmatrix} \begin{pmatrix} y_o \\ 0 \end{pmatrix}$$

from which $\dot{y}_1 = M_{21} y_o$ (where y_o is in units of d).
Then $\theta = \left| M_{21} \right| \frac{y_o}{d}$ where y_o is in cm.

For reasons which will be made clear later, it is also of interest to have an expression for the amplitude of the trajectory in the x - z plane at a distance a from the lens exit. This may be found as follows: the transformation consists of a lens followed by a drift space of length a. Hence:

$$\begin{pmatrix} x(a) \\ \dot{x}(a) \end{pmatrix} = \begin{pmatrix} 1 & a \\ 0 & 1 \end{pmatrix} \begin{pmatrix} N_{11} & N_{12} \\ N_{21} & N_{22} \end{pmatrix} \begin{pmatrix} x_o \\ 0 \end{pmatrix}$$

from which $x(a) = (N_{11} + aN_{21})\, x_o$.

Similarly, if the focus plane is a D. C. plane, we obtain:

$$S_y = -N_{11}/N_{21} \qquad S_x = -M_{11}/M_{21}$$

$$\theta = \left|N_{21}\right| y_o/d$$

$$x(a) = (M_{11} + aM_{21})\, x_o \quad .$$

The results of the calculations are presented below in graphical form for the two cases: (1) near-focussing (y - z) plane a C. D. combination, and (2) near-focussing plane a D. C. combination.

Curves are provided of the near-focus image distance S_y (measured from the exit of the second lens) versus lens strengths ω_1 and ω_2, with L, the lens separation and S_x treated as parameters. Data is provided for three values of L, namely:

$$L = 0.5,\ 1,\ \text{and}\ 2\ \text{(in units of d)},$$

however, only one value of S_x , $S_x = 500$ has been considered. (Calculation showed, as might be expected, values of ω_1, ω_2 to be rather insensitive to S_x for $S_x \gtrsim 500$.

Curves of θ/y_o (the ratio of the beam 1/2 angle of divergence to the initial 1/2 width in the near-focus plane) versus S_y are given, as well as curves of S_y versus x_1/x_o (the ratio of the beam 1/2 width at the lens exit to the initial 1/2 width, in the x - z plane).

In using these curves it should be noted that all dimensional quantities are given in units of d, the effective length of a lens element.

S_y vs ω_1 : y - z Plane a C. D. Plane

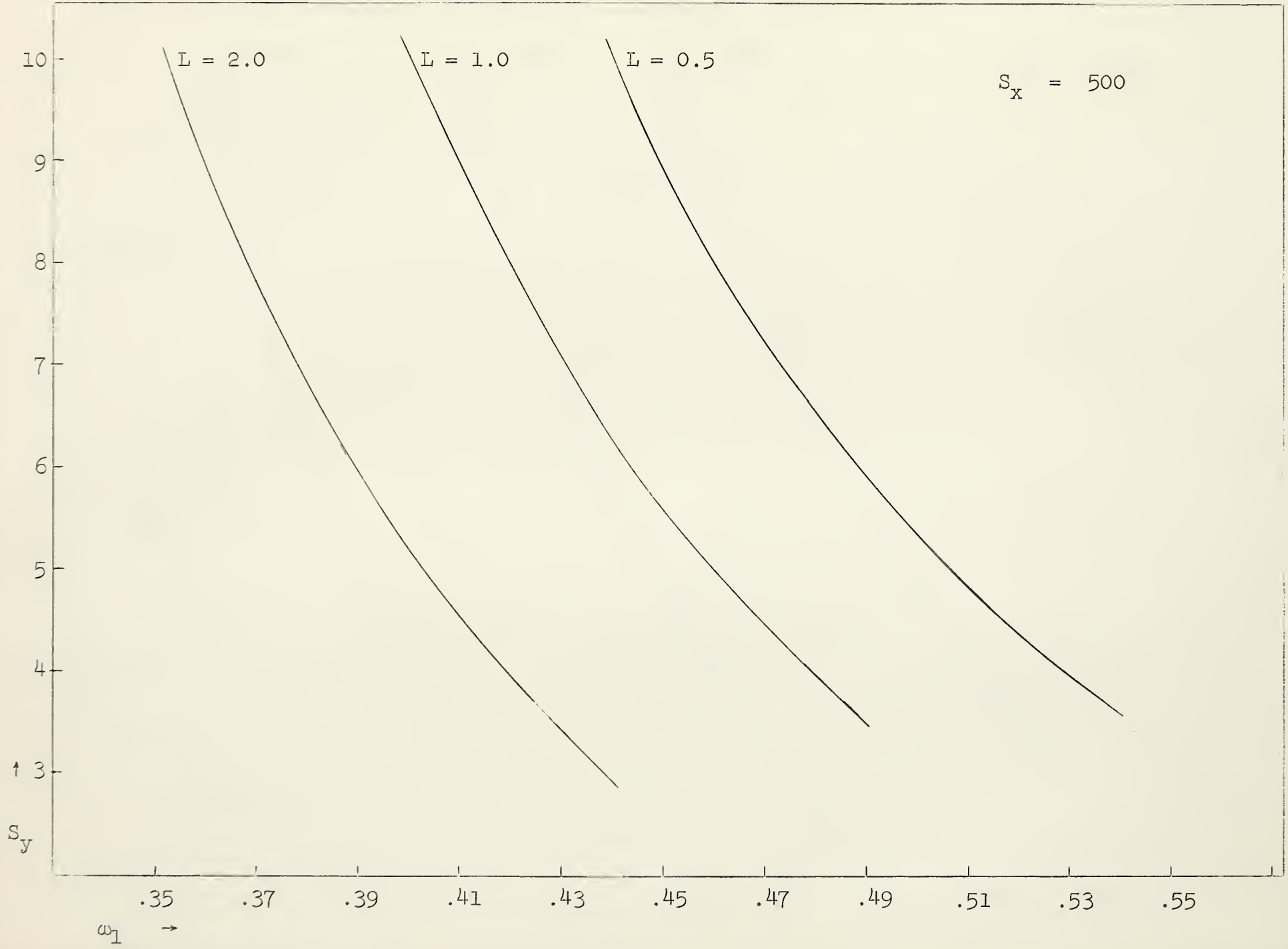

S_y vs ω_2 : y - z Plane a C. D. Plane

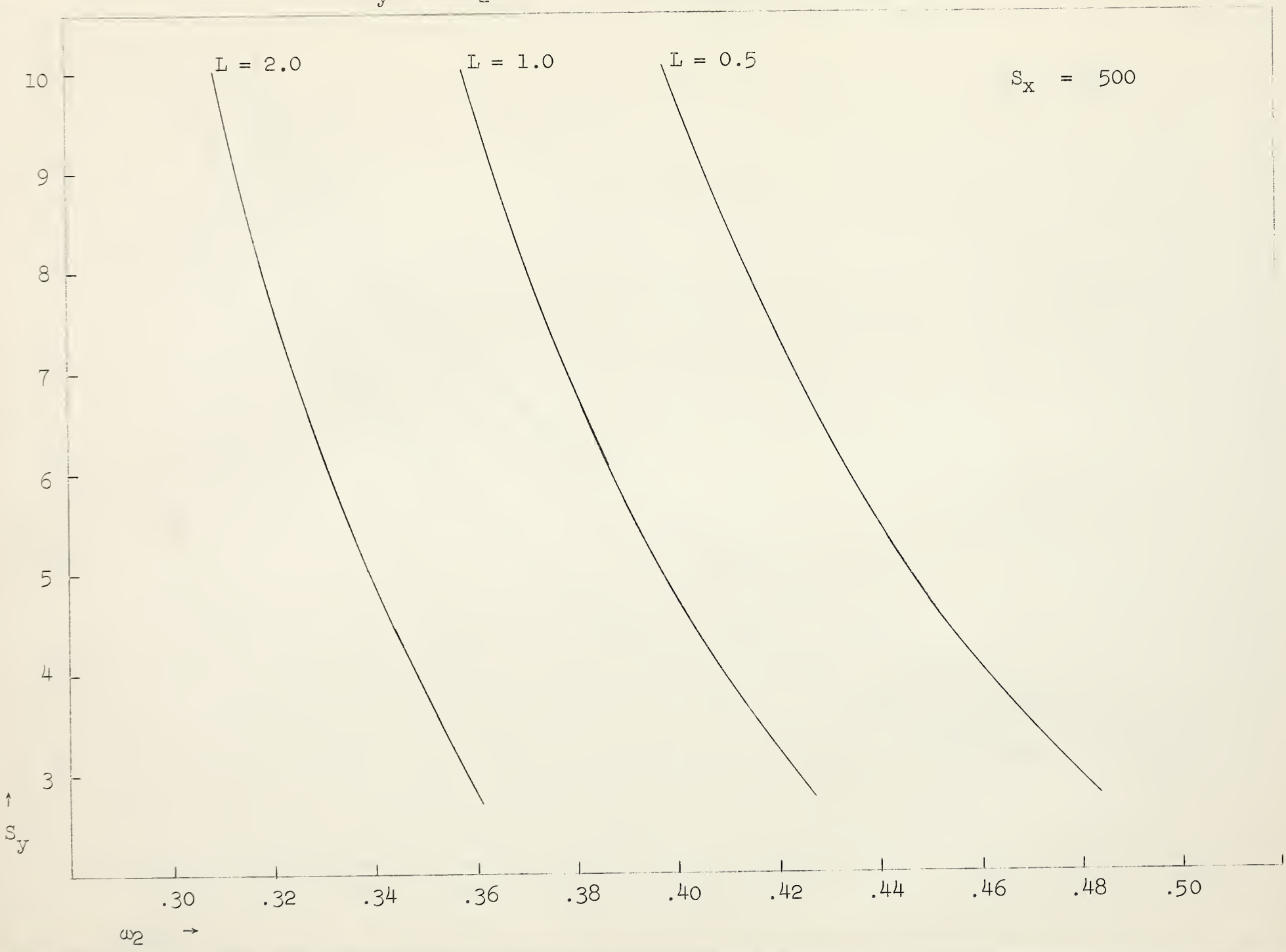

S_y vs θ/y_o : y - z Plane a C. D. Plane

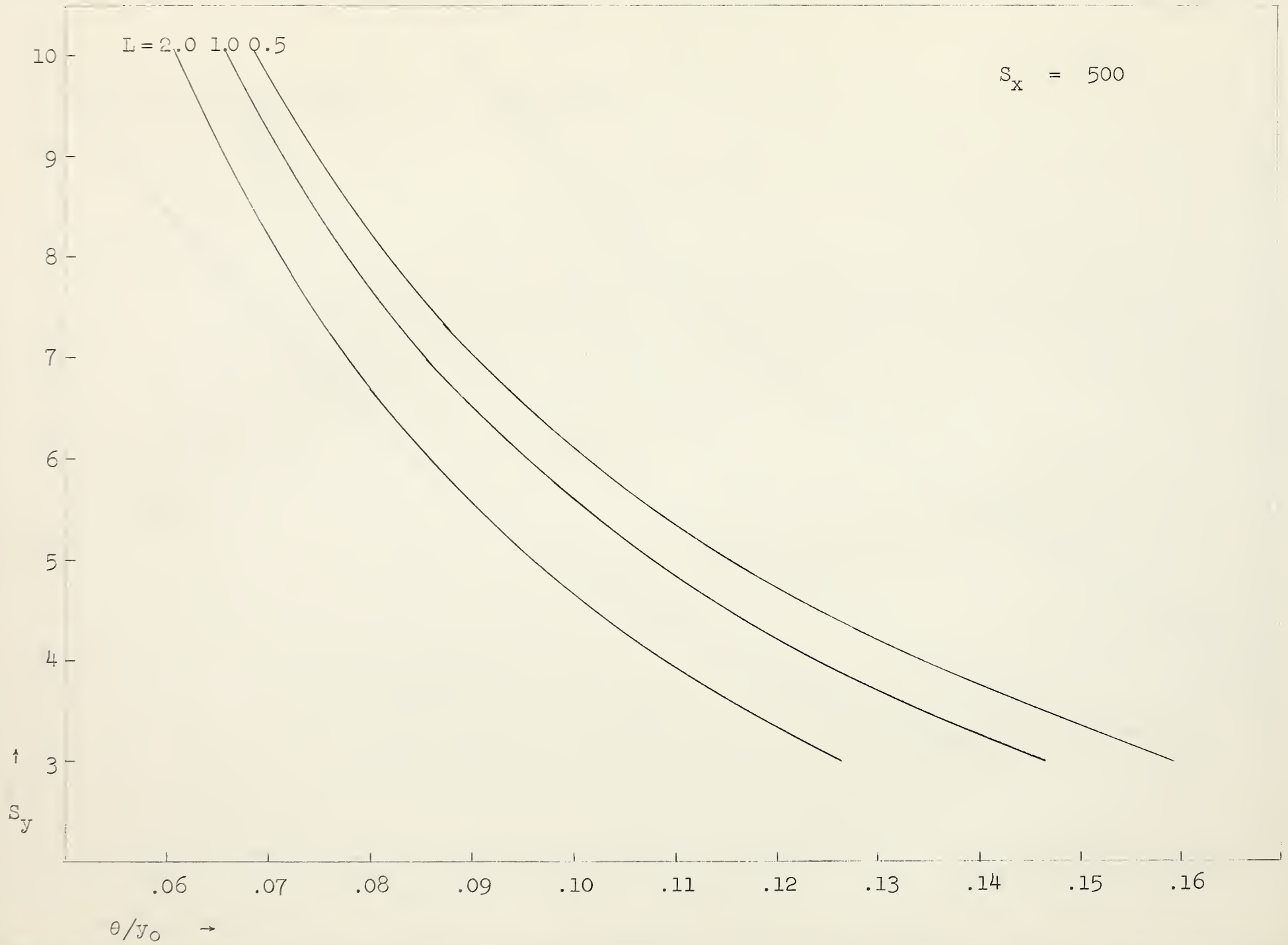

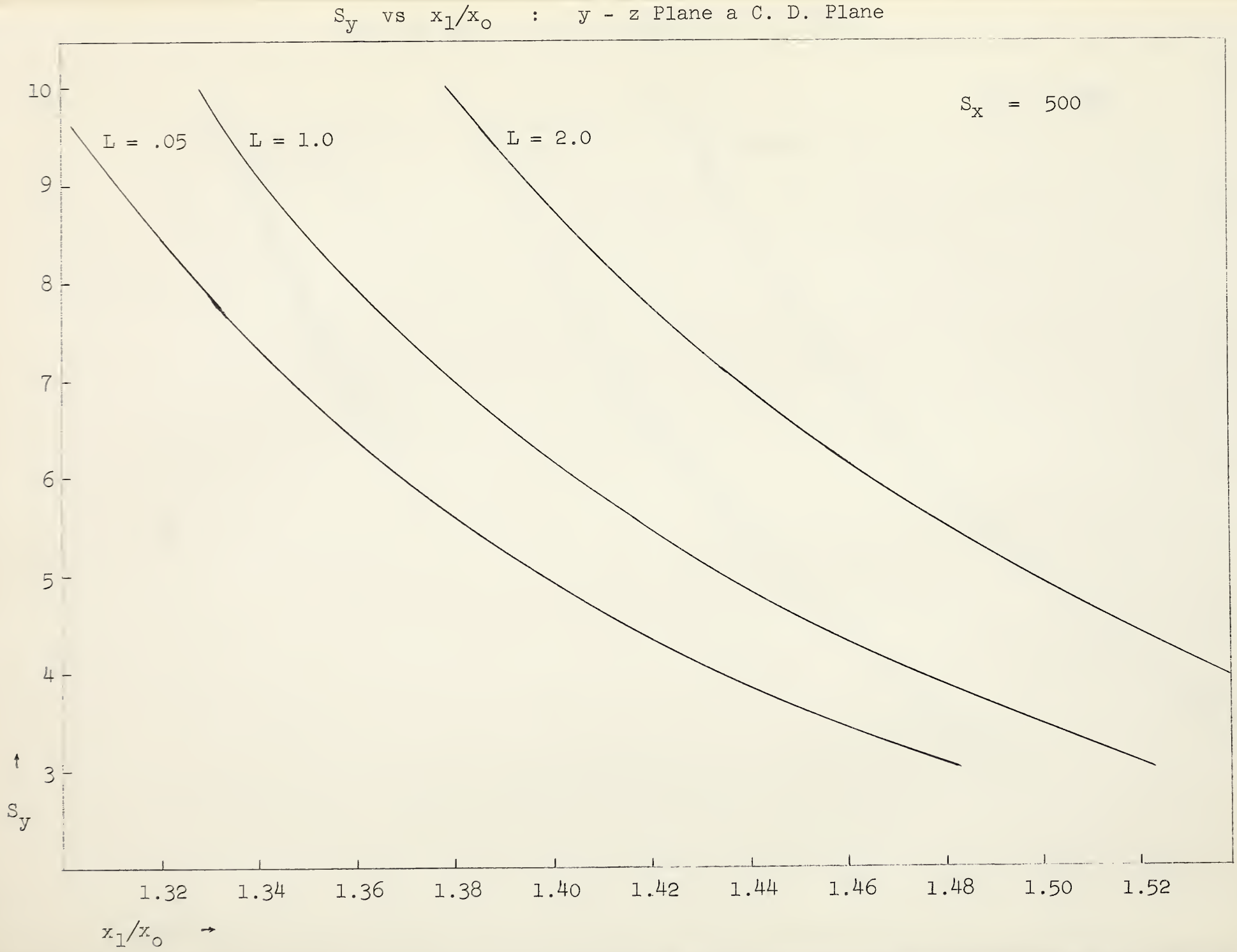
S_y vs x_1/x_o : y - z Plane a C. D. Plane
S_x = 500
L = .05
L = 1.0
L = 2.0
10
9
8
7
6
5
4
3
S_y
1.32
1.34
1.36
1.38
1.40
1.42
1.44
1.46
1.48
1.50
1.52
x_1/x_o

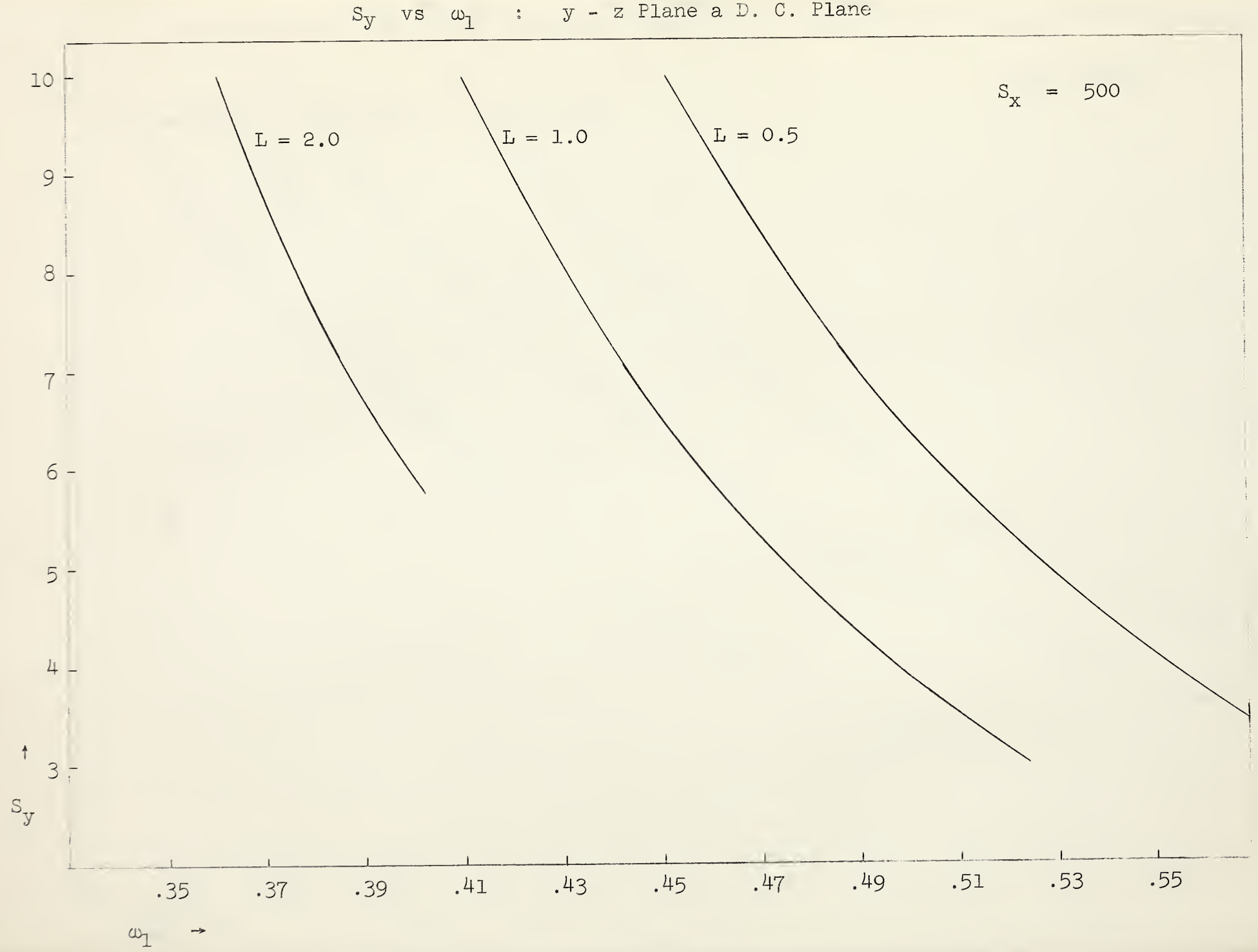
S_y vs ω_1 : y - z Plane a D. C. Plane
S_x = 500
L = 2.0
L = 1.0
L = 0.5
10
9
8
7
6
5
4
3
S_y
.35
.37
.39
.41
.43
.45
.47
.49
.51
.53
.55
ω_1

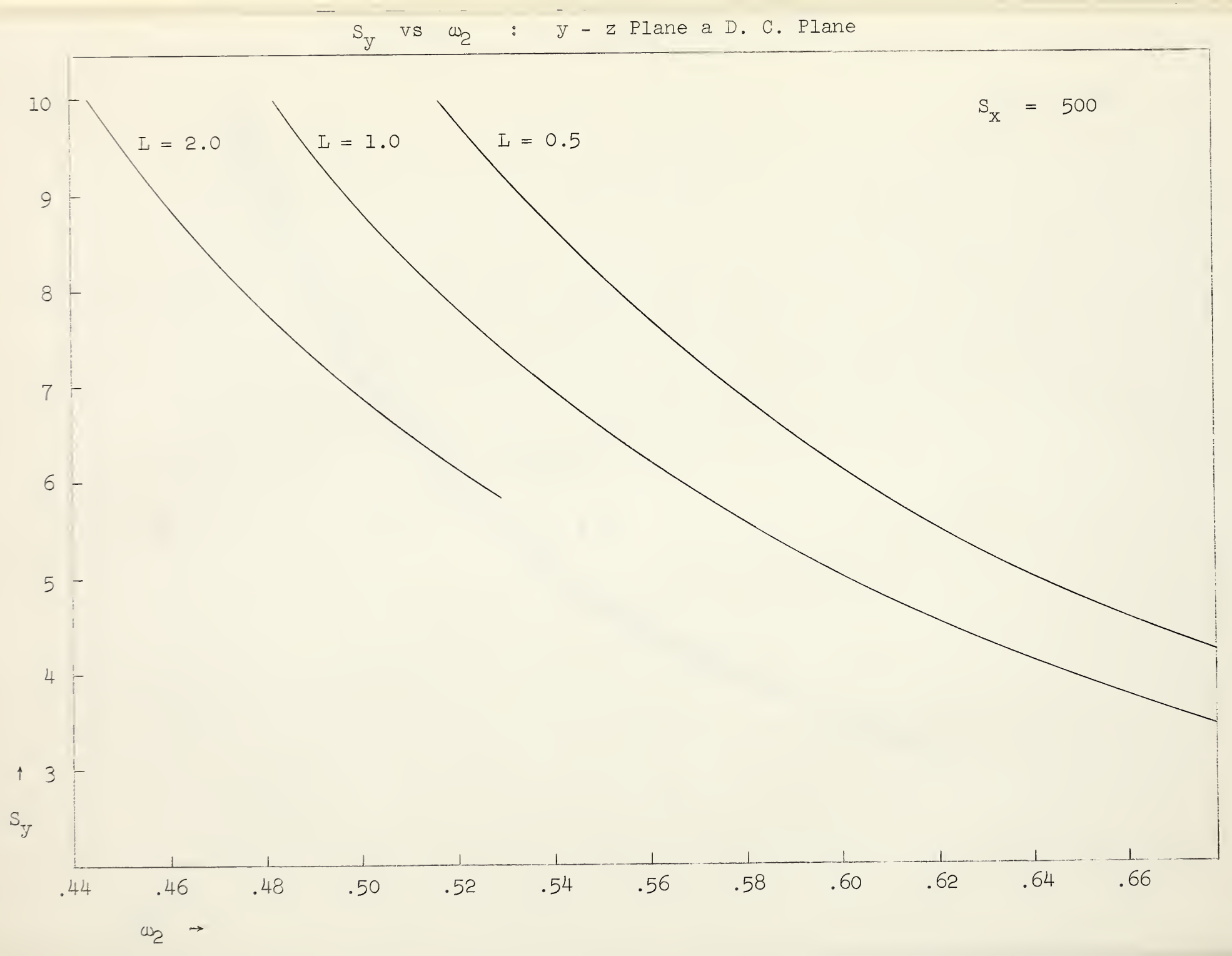
S_y vs ω_2 : y - z Plane a D. C. Plane
S_x = 500
L = 2.0
L = 1.0
L = 0.5
10
9
8
7
6
5
4
3
S_y
.44
.46
.48
.50
.52
.54
.56
.58
.60
.62
.64
.66
ω_2

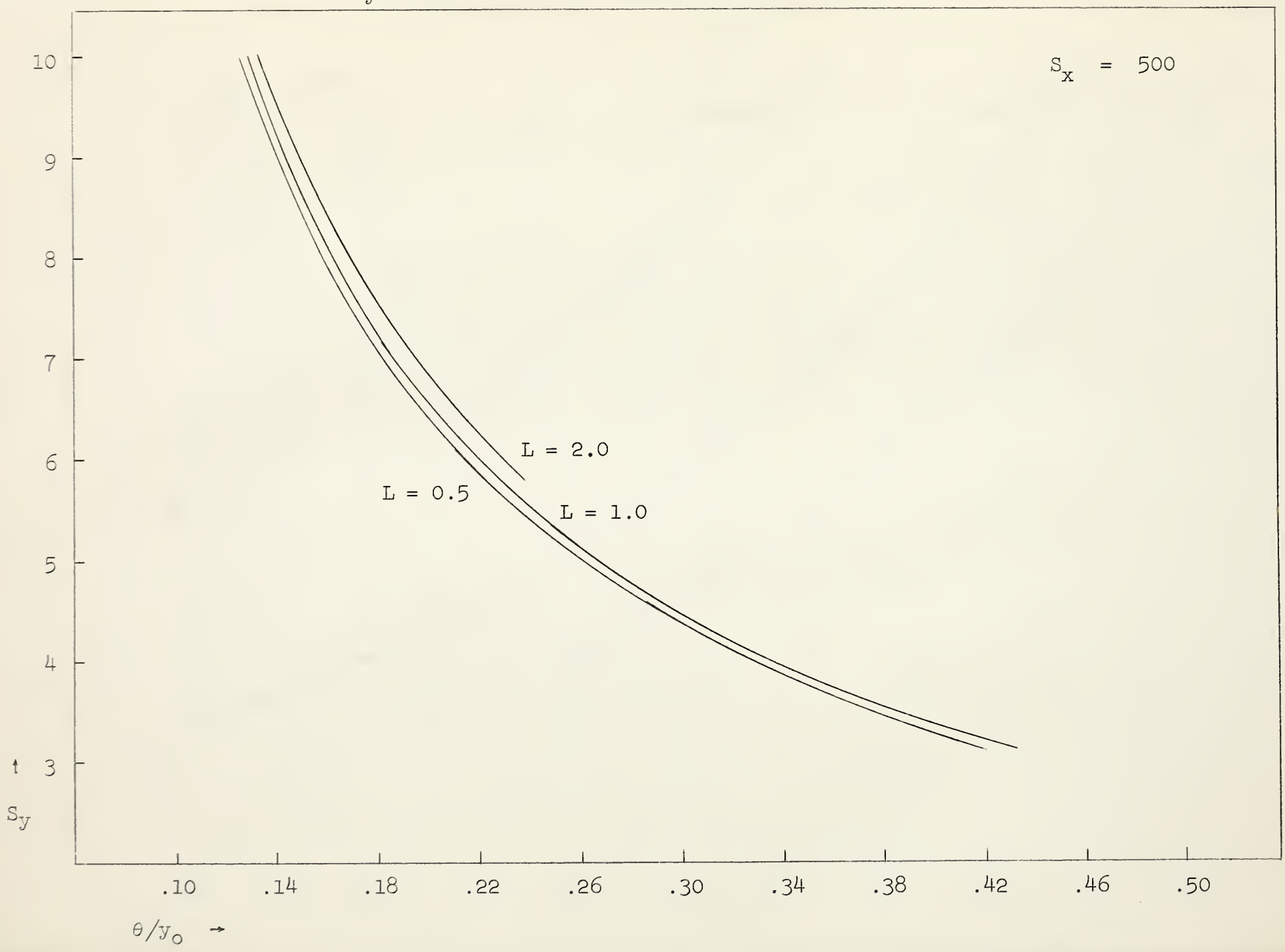
S_y vs θ/y_o : y - z plane a D. C. Plane
S_x = 500
L = 2.0
L = 0.5
L = 1.0
10
9
8
7
6
5
4
3
S_y
.10
.14
.18
.22
.26
.30
.34
.38
.42
.46
.50
θ/y_o →

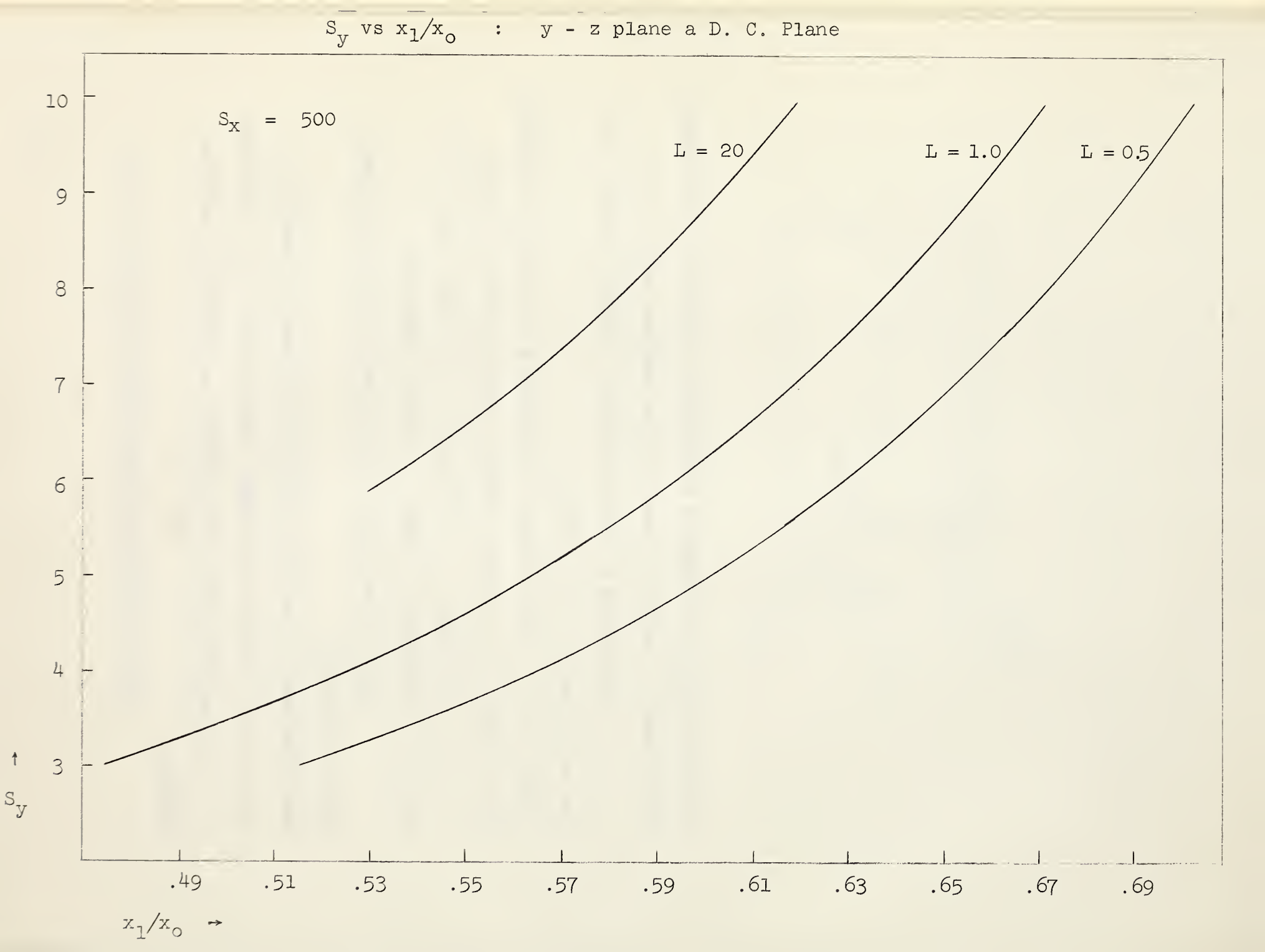
S_y vs x_1/x_o : y - z plane a D. C. Plane
S_x = 500
L = 20
L = 1.0
L = 0.5
10
9
8
7
6
5
4
3
↑
S_y
.49
.51
.53
.55
.57
.59
.61
.63
.65
.67
.69
x_1/x_o →

The following conclusions may be drawn from the graphs:

For given S_x, S_y, L, higher voltages are required in case (2) (see previous page) than in case (1). The maximum permissable beam half-length x_o is less in case (1) than in case (2).

With θ also fixed, the maximum initial beam half-width y_o is greater in case (1) than in case (2).

The effect of increasing L, the lens separation, is, in case (1) to permit larger values of y_o but smaller values of x_o. The situation is reversed in case (2) although the reduction in y_o is slight.

Increasing S_y permits larger values of both y_o and x_o in case (1) while in case (2) the maximum value of y_o increases while the maximum permissable value of x_o decreases.

III. DESIGN OF THE APPARATUS

A. The Quadrupole Lens System

There are a number of requirements on the shape and dimensions of the ion beam which bear on the design of the lens system.

As pointed out earlier, for maximum transmission through the mass spectrometer analyzer, the beam should be parallel or slightly convergent in the plane of the analyzer magnetic field. At the same time in the other plane (y-z plane), the beam must be sharply focussed at a relatively short distance from the lens exit.

From the following diagram illustrating the quadrupole pair mounted in the beam tube,

The Quadrupole Lens Mounted in the Beam Tube
Fig. IV

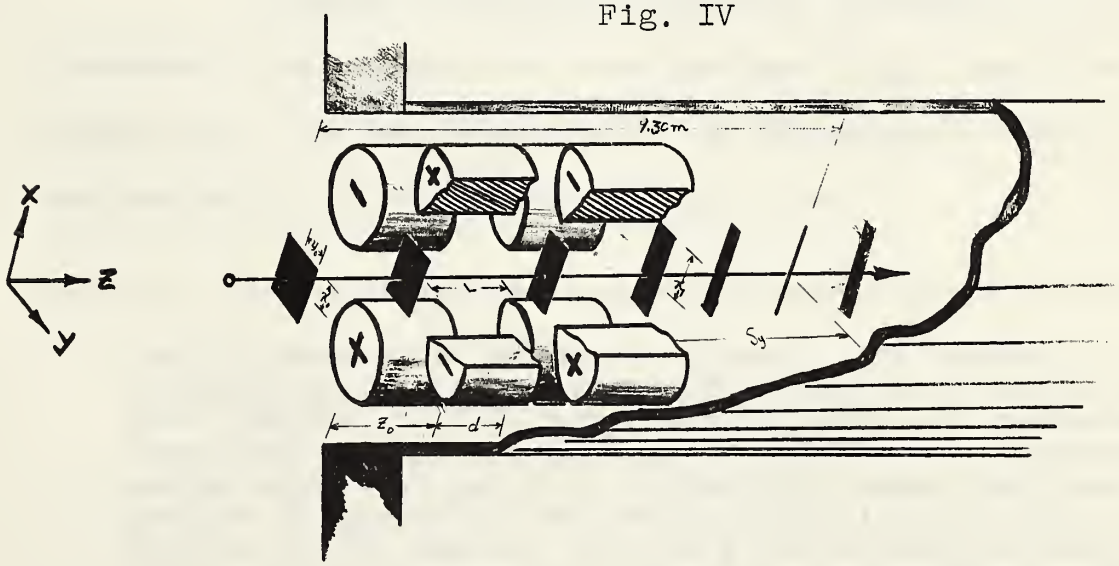

it is seen that $(S_y+z_o+2+L)d \leq 9.3$ cm.

Assuming an instrument possessing only first order focussing,* the resolution is give by

$$M/\Delta M \approx \frac{R}{S_s + S_c + \theta^2 R + \ldots}$$

where $\theta^2 R$ is the contribution due to spherical abberation in the analyzer magnet. In the present case, the collector slit width S_c = .017" while the radius of curvature R = 6". Thus the $\theta^2 R$ term is essentially negligible if

$$\theta \lesssim .02 \quad .$$

Since $\theta = M_{21}\, y_o/d$ (if y - z plane a C. D. plane) and since M_{21} is fixed by the requirements on S_y, S_x, the restriction on the value of θ may be considered a restriction on the value of y_o, the initial beam half-width.

In order to minimize spherical abberation in the quadrupole lens system the lens aperture ($2R_o$) should be much larger than the beam dimensions. In the present case, the maximum practicable aperture is $R_o \sim 6$ mm.

---

* The instrument for which the present lens system is intended has, in fact, specially shaped pole pieces such that ideally the $\theta^2 R$ term does not enter (ie.second-order focussing). However, as Barnard[1] points out, achieving second order focussing in a practical sense requires precise alignment of the source and collector slits with respect to the magnet. In the present circumstances, this would be extremely difficult to accomplish owing to a lack of knowledge of the precise position of the source defining "slit" (ie. crossover point).

Upper limits on the intial half-width of the beam in the x - z plane are set by the obvious requirement that transmission losses as a result of the beam being obstructed by the lens itself or by the spectrometer tube are to be avoided. This situation is furthermore undesirable on the grounds that bombardment of metal parts or insulators by the ion beam can lead to spurious effects due to polarization or secondary electron emission, as pointed out earlier. Thus we require:

$$x_o \leq R_o = 6 \text{ mm}$$

$$x_1 = N_{11}x_o \leq R_o = 6 \text{ mm} \quad \text{(if y - z plane a C. D. plane)}$$

$$x(a) = (N_{11}+N_{21}\frac{a}{d})x_o \leq 5 \text{ mm}$$

We have thus established criteria for the upper limits on x_o, and y_o. Lower limits are set by the requirements of sensitivity. In the conventional source used in this laboratory the aperture next to the filament has an area of 16 mm^2 and hence we may require

$$x_o y_o \gtrsim 4^2 \text{ mm}.$$

From the graphs, the following data are obtained (assuming $z_o = 1.5$ mm, $d = 1.3$ cm, $R_o = 6$ mm, $\theta_{max} = .02$ rad., $x(a)_{max} \approx x_{1max} = 4$ mm.)

Design Parameters for Quadrupole Ion Source

	Lens Combination in near-focus (y-z) Plane	Lens Separation L (in units of d)	Image Distance S_y (in units of d measured from effective lens exit)	Voltage on first lens V_1 (in units of E, the beam energy)	Voltage on second lens V_2 (in units of E, the beam energy)	Maximum initial beam half-width y_o (in mm)	Maximum initial beam half-length x_o (mm)	Maximum initial beam cross-sectional area (mm^2)
	C. D.	2	3.04	$\pm$ .041	$\pm$ .027	2.06	2.53	20.8
	C. D.	1	4.04	$\pm$ .049	$\pm$ .036	2.12	2.72	23.1
a)	C. D.	0.5	4.54	$\pm$ .056	$\pm$ .043	2.12	2.80	23.8
	D. C.	1	4.04	$\pm$ .053	$\pm$ .089	0.78	7.88	23.7
b)	D. C.	0.5	4.54	$\pm$ .062	$\pm$ .094	0.90	6.84	24.6

To take advantage of the slightly larger maximum initial beam area a lens separation of L = 0.5 was chosen.

Two sizes of defining slits were made with dimensions appropriate to maximum area in cases (a) and (b). This was done to check the extent of abberations in the system.

The physical dimensions of the quadrupole parts are given in the drawings of Section (c) below.

B. The Ionization Chamber and Accelerator

Several arrangements for obtaining a parallel beam as input to the quadrupole lens were tested. All of these consisted of a stack of circular rings separated by equal potential intervals preceded by an ionization chamber with associated electrodes.

The first arrangement tested consisted in the following:

Fig. V

Schematic: Ionization Chamber and Accelerator

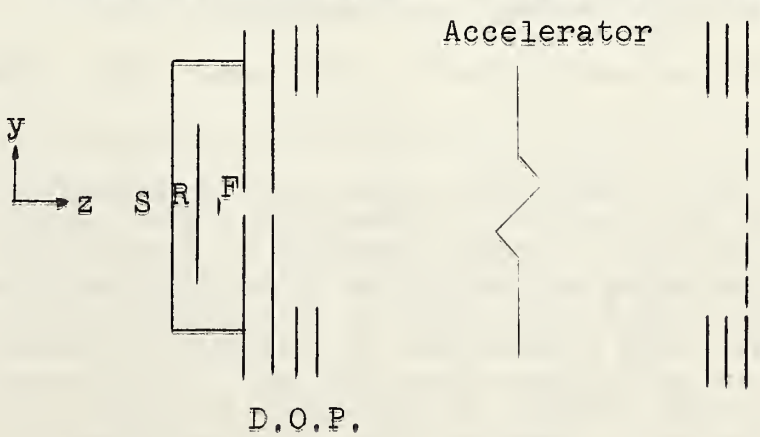

The ionization chamber was identical with that used in the conventional source, with the exception of the aperture dimensions. A repeller electrode as well as provision for adjusting the case potential with respect to the filament were provided. The drawing out plate was variable in potential from that of the case to that of the uppermost accelerator electrode and had an aperture of dimensions equal to the maximum permissable initial beam dimensions. The uppermost plate of the accelerating section had an aperture of the same dimensions as the remaining accelerator electrodes. The final plate of the accelerator held a tungsten wire grid the purpose of which was to terminate the accelerator field. (Penetration of the accelerator field into the region of the quadrupole lens would produce chromatic abberations in addition to defocussing the beam). In order to minimize beam scattering in the focus plane the grid was constructed with wires running perpendicular to the long axis of the beam cross over (ie. parallel to the y-axis).

The arrangement was tested using a fluorescent screen*. For these tests, Cesium ions emitted from a

---

* Fluorescent screens were deposited on the end of a glass cylinder which was waxed to a steel flange, the latter being bolted to another flange on the ion source. Screens were constructed by settling the phosphor on glass previously coated with a conducting film. Materials and recipe for depositing the screens were from the Sylvania Corporation. The tin oxide conducting coating was deposited using the technique of Gomer[11] Electrical contact to the flange was made with Aquadag. The Aquadag was also extended along the walls of the tube to within approximately 1/4" of the screen.

Rhenium filament were used. Cesium has a low ionization potential while Rhenium has a high work function, thus considerable ionization is produced at relatively low temperatures. Low temperatures are required in order not to obscure the image of the beam with light from the filament. The images produced using such filaments always appeared to be incomplete, ie. sections of the pattern were missing while some sections were brighter than others. This appears to have been due to non-uniform emission from the filament, probably the result of a non-uniform distribution of the Cesium salt on the filament.

The arrangement did not appear capable of producing a well defined parallel beam of rectangular cross-section. However, tests were rendered inconclusive owing to uncontrollable flash-over on the fluorescent screen. Eventually screens were constructed which did not flash-over*,

---

* The flash-over problem seems to have been due to excessive resistance between screen and ground. Applying thicker tin oxide coatings (enough to produce a milky discoloration on the glass) in addition to extending the coating over almost the entire inner surface of the glass tube seemed to be helpful in one case. However, using C_S^+ ions, some flash-over (controllable) still occurred for large enough current. On the other hand, with electrons on the same screen, no flash-over occurred, even at much higher currents. The enhanced electron mobility in the screen material might account for this. The difference in secondary electron emission in the two cases might also be significant.

however, the original arrangement was not tested on these screens. The original tests had indicated the need for further beam shaping. It was also felt that some provision for focussing the beam slightly, previous to entrance into the accelerating section as well as provision for beam centering previous to acceleration might be helpful.

To accomplish this, a Nier type thick lens[5] was used. In addition, defining slits were placed at the entrance and exit (following the tungsten wire grid) of the accelerator section. The following schematic illustrates the situation.

Schematic - Alternate Arrangement Using Nier Type Thick Lens

Fig. VI

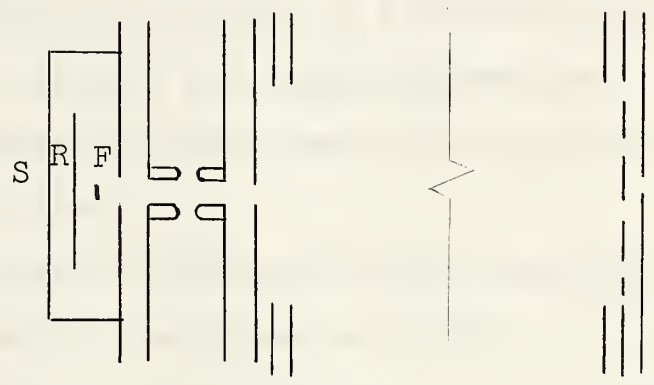

The plates D. O. P. and Focus together comprise the Nier type thick lens. A detailed ray-tracing for such a lens has been carried out by Dietz[5] who gives data

appropriate to the case where strong focussing is required. These data were used as a guide in determining empirically, with the fluorescent screen, the lens voltages appropriate to the present case.

Beam centering was provided by making the focus plate a split plate.

Results obtained using this arrangement are discussed in Chapter IV.

C. Construction of the Source

All metal parts were of stainless steel (#304), chosen for its non-magnetic qualities in addition to relative ease of finishing. All electrode surfaces in contact with the beam were polished to a mirror finish to reduce polarization effects and degassing problems.

Insulators which serve as spacers for the electrodes were made of Lava*.

Critical dimensions on all Lava and metal parts were machined to a tolerance of .001".

The method of mounting the quadrupole electrodes will be clear from the drawing. The remaining electrodes were mounted on four 1/16" diameter stainless steel posts

---

* Talc. The material is soft and easily machinable to normal tolerances when raw. After machining, the part is baked in a hydrogen atmosphere. The resultant piece is extremely hard and tough. Some shrinkage occurs during baking. However this is quite uniform and hence is easily compensated.

threaded into the rear face of flange # 1. 3 mm. glass tubing placed over the posts insulated them from the electrodes. Electrode plates had holes drilled in them to receive the glass covered posts. This type of construction is identical with that used in the conventional source.

The accelerator section consisted of twenty identical rings joined by Pyrofilm PT 500 glass covered resistors (500 K $\pm$ 1%). One lead of each resistor was spot-welded to an electrode. The other lead passed through a hole drilled in the plate above. Electrical connection was assured by simply bending the leads to provide a slight tension.

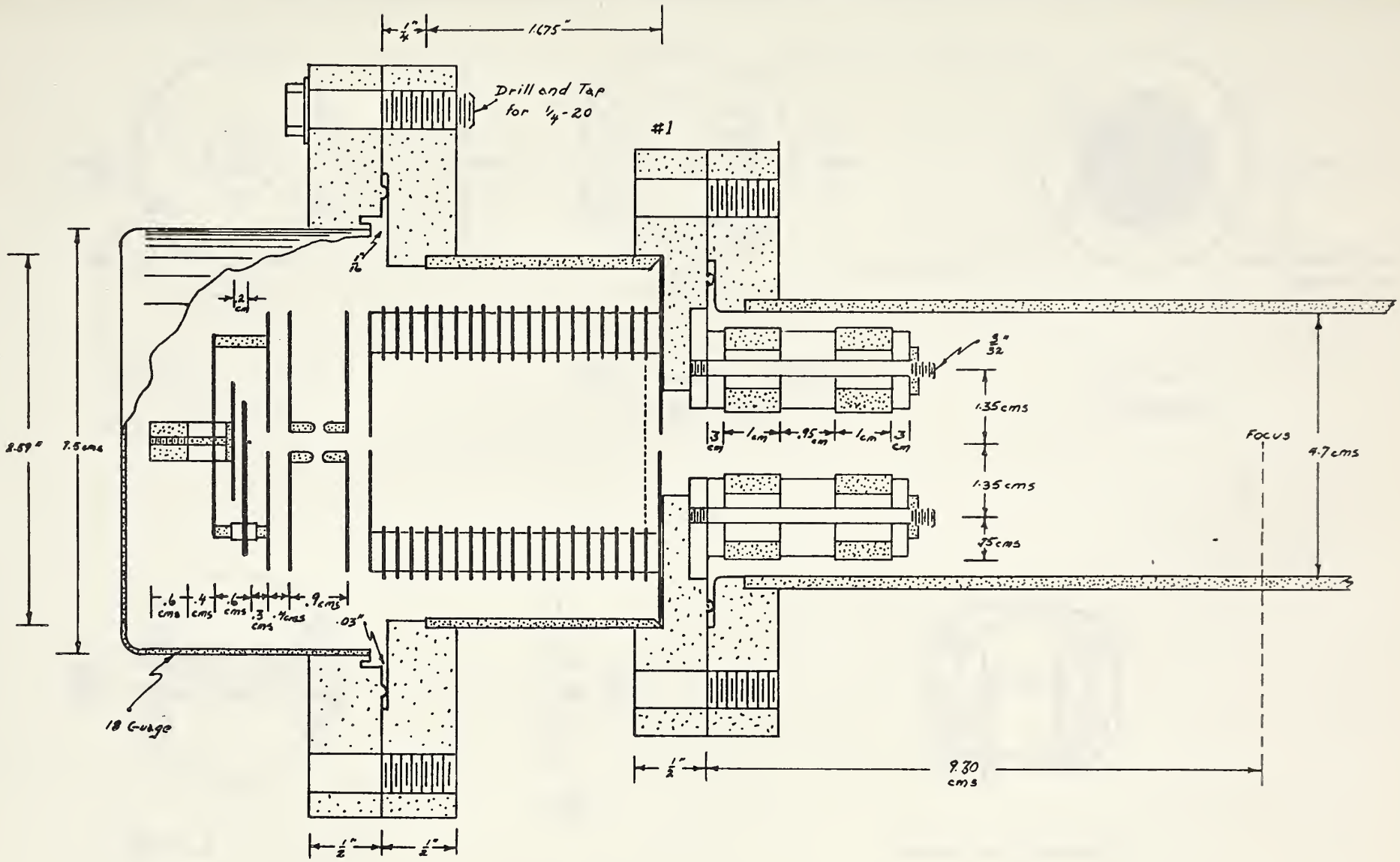

PROFILE : QUADRUPOLE LENS SOURCE FOR MASS SPECTROMETER

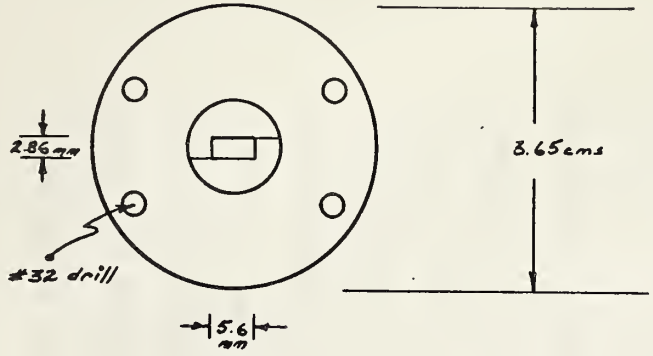

Defining Slit
(.025" S.S.)

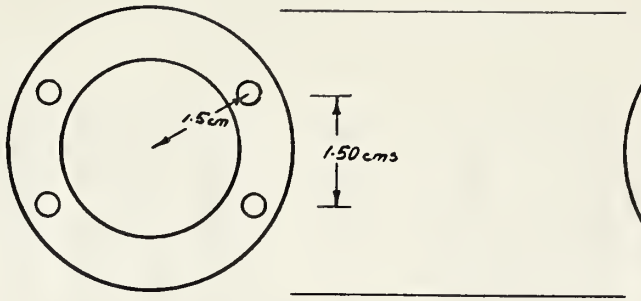

Accelerator Rings
(.025" S.S.)

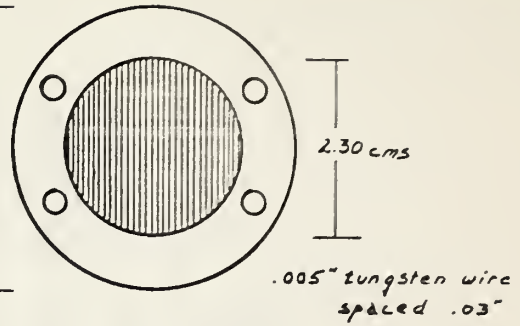

Grid
(.025" S.S.)

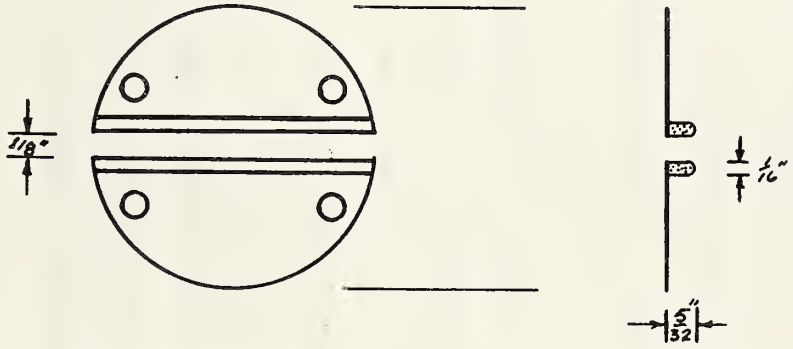

Plates for Nier
Thick Lens

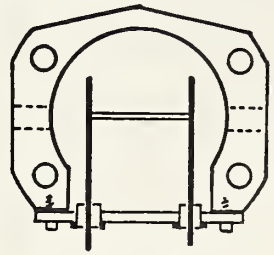

Ionization Chamber

ELECTRODES

IV. RESULTS

The device was set up with a fluorescent screen mounted as closely as possible to the required cross-over position. For these tests, the source was operated with reversed electrode potentials using the Re filament as an electron emitter. This proved to be far more satisfactory than using Cs^+ ions as was done initially. Complete patterns of more than adequate intensity were obtained.

A variety of defining slit widths were tried in order to indicate the extent of any abberations.

Using defining slits .030" x .40" and with the focussing plate shorted to the D. O. P. (ie. with no focussing action from the thick lens) a sharply defined rectangular pattern approximately .13" x .8" was obtained on the fluorescent screen. In spite of the divergence of the beam, a very sharp line focus approximately .010" wide was obtained with the quadrupole lens turned on. With the focus plate unshorted and the potentials readjusted to give a parallel beam a very poorly defined rectangle of approximately the dimensions of the defining slit was obtained. The pattern was of much greater intensity than that obtained in the previous case (a factor of about 10, as determined later with the source mounted on the mass spectrometer). However, when attempts were made to focus this pattern with the quadrupole lens, line widths of no better than approximately

.020" were obtained. Moreover, the line focus had rather diffuse edges.

The quality of focus obtained in both cases tended to be quite sensitive to changes in the voltages applied to the D. O. P. and Focussing electrodes. A much more serious problem, however, was that changes in these electrode voltages generally tended to move the beam laterally. Both effects are almost certainly due to misalignment of the electrodes. Unfortunately, with the type of mounting used little can be done to correct this.

Some focussing in the x - z plane also occurred for certain values of the focus voltage. However, this could not be controlled in a desirable fashion and hence was a detriment. The effect was probably caused by using a defining slit as top plate of the accelerator adjacent to the split focus plate. With a defining slit of finite length field gradients in the x - z plane would be set up.

The apparatus was next mounted on the mass spectrometer. With a filament loaded with Rb_2SO_4 the task of aligning the instrument was begun. This proved to be both tedious and difficult.

Complications arose for a variety of reasons. When the filament was removed for reloading slightly different potentials were required on the electrodes owing presumably to the impossibility of repositioning the fila-

ment precisely. Normally this would not be relevant but in the present case some lateral displacement of the beam results, as was pointed out above. In addition some changes in beam divergence must occur with the result that the axial position of the line focus is shifted. The net result is that it is practically impossible to know the exact location of the line focus.

The following sketch illustrating the requirements of alignment will serve to indicate the nature of the problem.

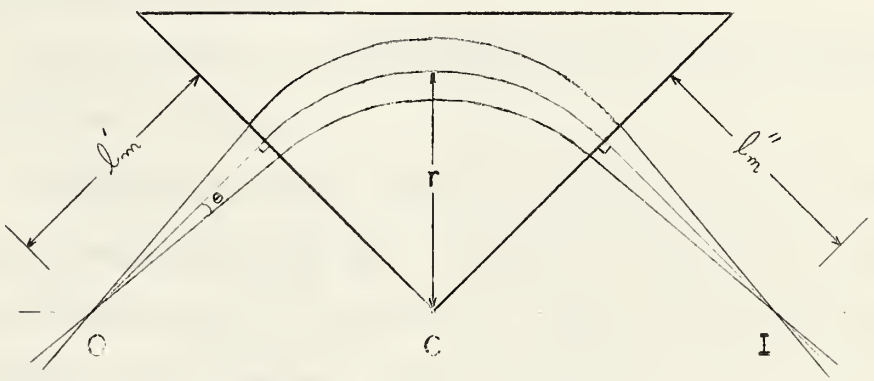

Source Slit (Cross-over Point)

Collector Slit

For a symmetric arrangement $\ell_m' = \ell_m''$. With the principal ray normal to the field boundaries the condition for refocussing is that the object, the centre of curvature, and the image lie on the same straight line[4].

Ultimately, a reasonable alignment was achieved by estimating the resolution of two mass peaks displayed on a pen recorder after each adjustment. No attempt was made to align the axis of the collector slit with that of the object line focus. Resolution was estimated by taking as peak width the distance at baseline between "best-fit" straight lines drawn along the sides of the peaks. In the present case (defining slits .030" and .40", S_C = 0.017", r = 6") a resolution of approximately 190 was obtained. (Fig. VIII). This value is most probably an under estimate since it assumes a constant scan rate, whereas, in fact, the scan rate varied exponentially.

An estimate of the beam width at the collector may be obtained as follows:

Consider an ideal beam of uniform current density and sharply defined width S_B. If such a beam be scanned over a collector slit of width $S_C > S_B$ an idealized peak shape results. The dotted curve shows the effect of distributed current density.

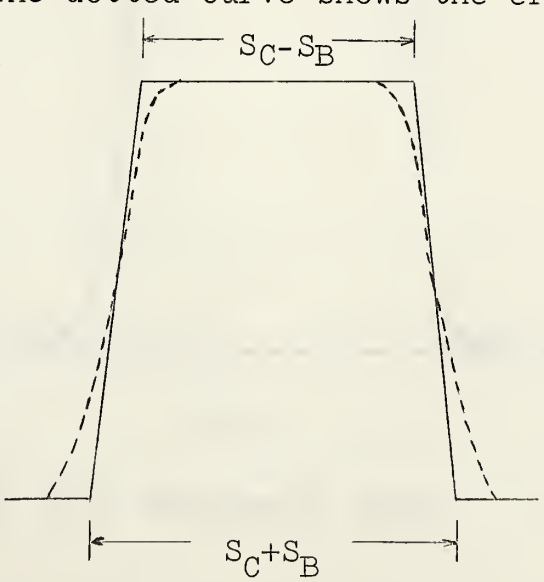

Figure VII shows a typical slow speed scan obtained under conditions previously noted. Applying the above considerations we find

$$S_B \approx .009"$$

as the beam width at the collector, and using

$$R = \frac{M}{\Delta M} = \frac{r}{S_B + S_C}$$

we find $R \approx 230$

Fig. VII

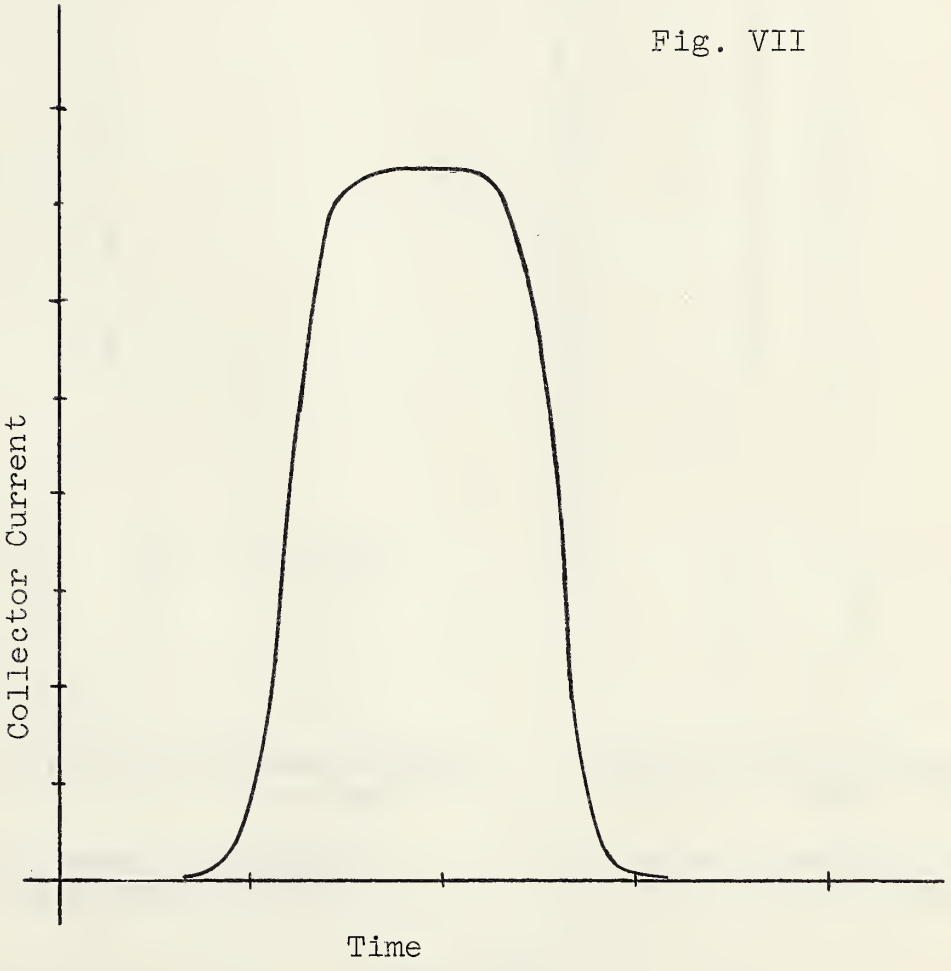

Peak Obtained with Quadrupole Source - Slow Speed Scan

By differentiating one side of the peak (Fig. VII) a current density profile of the ion beam at the collector may be obtained. (Fig. VIII, a) this should be compared with Fig. VIIIb which shows results obtained with the conventional source.

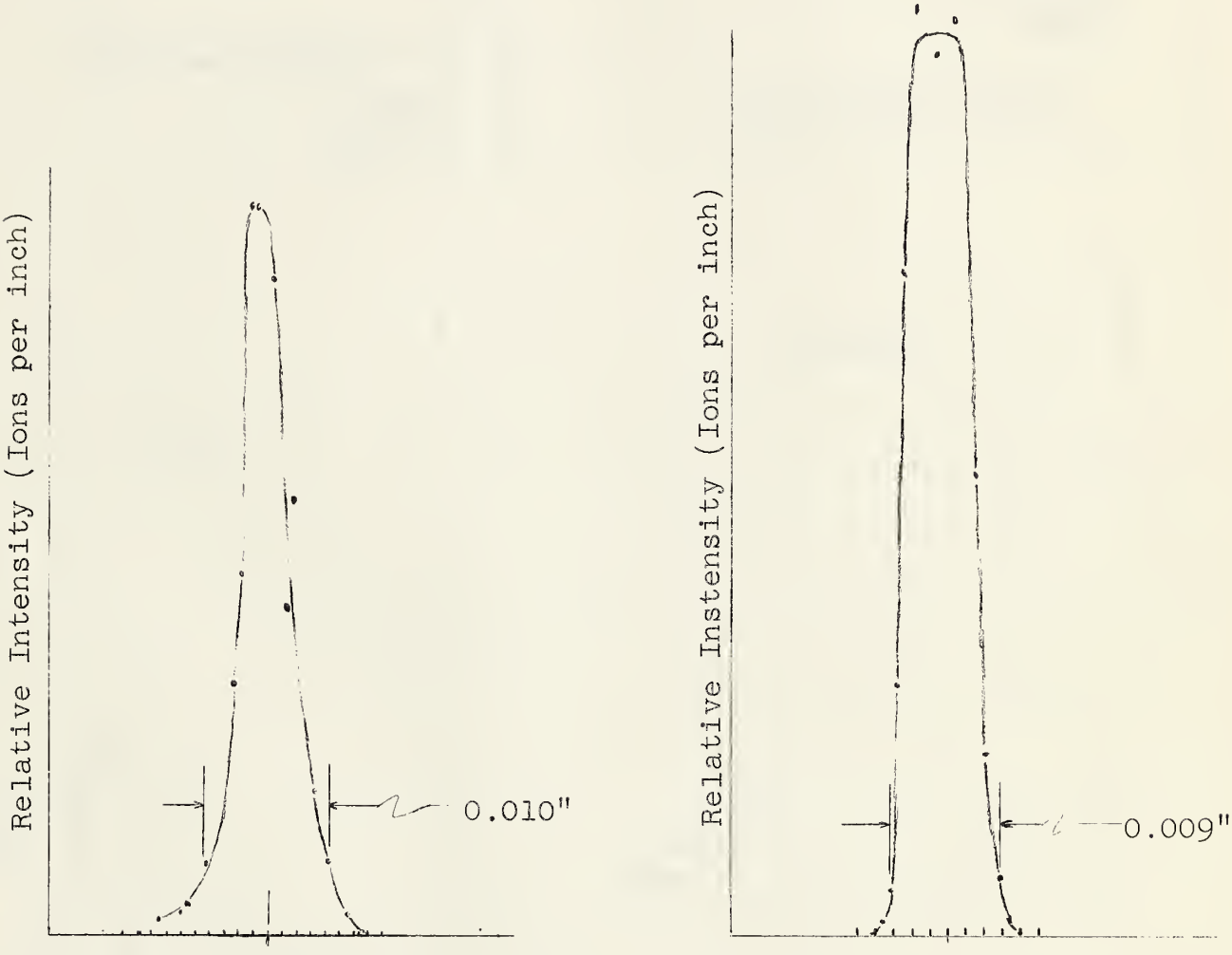

a) Current Density Profile: Quadrupole Source

b) Current Density Profile: Conventional Source

Fig. VIII

Fig. IX shows, for comparison, Rb peaks obtained with the quadrupole source along with a similar set obtained with the conventional source.

Fig. IX - Comparison of Rb Peaks

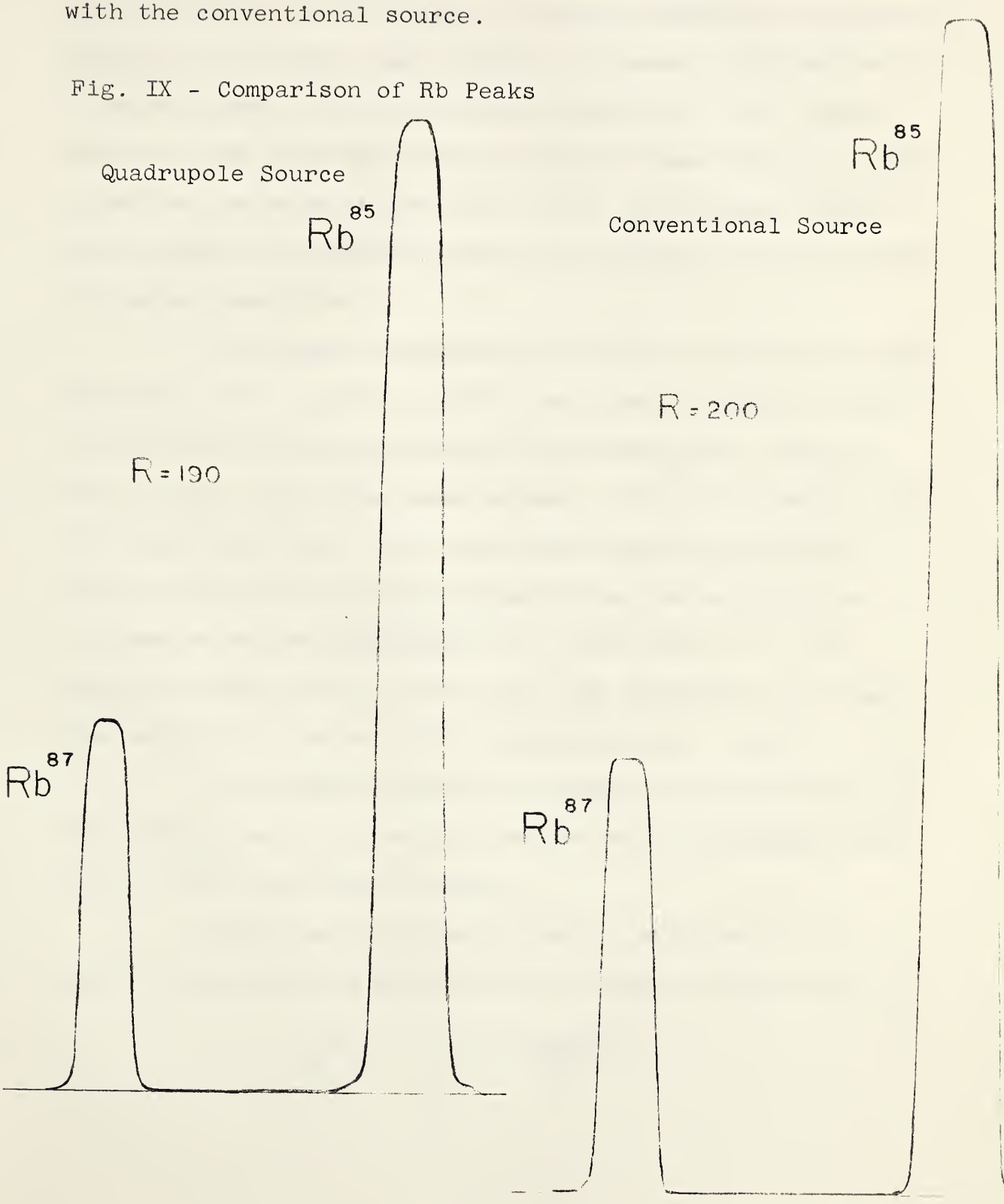

It will be noted that the peaks obtained with the quadrupole source exhibit less resolution than those obtained with the conventional source. Moreover, greater "tailing" is shown in the former case. Partly, at least, this may be due to misalignment of the source and collector "slit" axis. However, work with the screen indicated some distortion and spread of the ends of the line focus. The effect, which would appear on recorder traces as "tailing", was due to the focussing electrodes.

The present arrangement was also tested using wide defining slits (.166" x .224"). As might be expected, the various abberations previously noted were again observed and, in fact, were much more marked. With no focussing from the Nier thick lens the accelerator section produced a sharply defined but badly divergent beam which could be focussed with the quadrupole to a line width of ~ .011". Using the Nier lens to remove the beam divergence the best line width obtained with the quadrupole was ~ .030".

An attempt was made to compare the sensitivity of the quadrupole source using this electrode arrangement with that of the conventional source.

Recalling that the ionization efficiency for positive ions emitted from the hot filament is given by

$$N_+/N_o = \exp\left[\frac{e(\omega-\varphi)}{kT}\right]$$

it is evident that a reasonable sensitivity comparison requires that ions be emitted at the same temperature in both cases. In addition, the work function of the filaments must be the same. These conditions were met as well as possible by using the same filament in both sources.

The measurements indicated an improvement in sensitivity by a factor of about 3 over the conventional source. This figure should perhaps be considered a lower bound on the true value since we can not be sure that the optimum focussing conditions for the quadrupole source were actually obtained.

V. REMARKS

The improvement in sensitivity obtained with the quadrupole source is not as high as reported by Kinzer and Carr who state that currents approximately 100 times higher than experienced with a conventional Winn - Nier gas source were obtained. It will be realized, of course, that such a figure is highly dependent on the detailed nature of the source being compared. Other workers suggest a factor of about 8.

The width of line focus obtained is not as narrow as had been hoped. However, the result is consistent with that reported by Giese, who obtained line widths of ~ .025" using an entering beam .375" wide. Both width of line focus and extent of "tailing" appear to be better than results obtained by Kinzer and Carr, as a comparison of Fig. VIII with their Fig. 2 would suggest.

Line widths of approximately .010" were obtained with the beam initially divergent and hence strongly collimated by the exit defining slit of the accelerating section. However, in all cases tested, attempts to produce an initially parallel entering beam always produced a line focus approximately twice this width. In addition, the line focus tended generally to be less well defined. The residual width appears to have been due partly to abberations in the pre-acceleration focussing lenses and partly to the grid used to terminate

the uniform field accelerating section.

It thus seems advisable to provide a final defining slit as in the conventional source. Transmission through such a slit would be quite large, and certainly higher than could be obtained with conventional focussing. The use of a defining slit would also considerably alleviate the problem of alignment of the source with the mass spectrometer.

BIBLIOGRAPHY

1. Barnard, G. P. - Modern Mass Spectrometry
2. Bullock, M. L. - Am. J. Phys. 23, 264
3. Courant, E. D., Livingston, M. St., and Snyder, H. S. - Phys. Rev. 88, 1190
4. Duckworth, H. E. - Mass Spectroscopy
5. Dietz, L. F. - Rev. Sci. Instr. 30, 235
6. El-Kareh, A. B. - Rev. Sci. Instr. 32, 423
7. Elmore, W. C. and Garrett, M. W. - Rev. Sci. Instr. 25, 480
8. Enge, H. A. - Rev. Sci. Instr. 30, 248
9. Enge, H. A. - Rev. Sci. Instr. 29, 885
10. Giese, C. F. - Rev. Sci. Instr. 30, 260
11. Gomer, R. - Rev. Sci. Instr. 24, 993
12. Harnwell, G. P. - Principles of Electricity and Electromagnetism.
13. Hess, Brown, Inghram, Patterson, and Tilton - Mass Spectrometry in Physics Research
14. Inghram, M. G. and Chupka, W. A. - Rev. Sci. Instr. 24, 518
15. Inghram, M. G. and Hayden, R. J. - A Handbook on Mass Spectrometry.
16. Kennett, T. J. and Thode, H. G. - Phys. Rev. 103, 323
17. Kinzer, E. T. and Carr, H. - Rev. Sci. Instr. 30, 1132
18. Langmuir, I. and Kingdon, K. H. - Proc. Roy. Soc. A 107, 61
19. Reynolds, J. H. - Rev. Sci. Instr. 27, 928
20. Rosenblatt, J. - Nucl. Instr. and Methods 5, 152-155
21. Schneider, H. - Nucl. Instr. and Methods 1, 268-273
22. Teng, L. - Rev. Sci. Instr. 25, 264
23. Weidemann, W. - Nucl. Instr. and Methods 9, 347-353

APPENDICES

APPENDIX I

Shape of Polepieces

As shown above, the required fields are produced by infinite hyperbolic pole pieces. Since this is impracticable and, in any case, hyperbolic forms are extremely difficult to machine, some approximate shape must be substituted. For ease of machining, cylindrical pole pieces are generally used. Satisfactory approximation to the hyperbolic shape is obtained if the cylinders have radius R' where:

$$1.125\ R_o < R' < 1.15\ R_o \qquad 19$$

where $2R_o$ is the lens aperture.

As shown by El-Kareh[6] and also by Elmore and Garrett[7] the term following the hyperbolic term in the power series expansion for a quadrupole potential of this symmetry is sixth order. Hence using cylinders to approximate the required form should introduce negligible abberation.

The calculations also assume square-shaped fields extending over a sharply defined region of length d. Calculations with the more realistic "bell" shaped fields give results which differ by approximately only 1% from those obtained in the present approximation.[20] The fringe fields may be accounted for by taking for the effective length of a lens element:

$$d = d' + \alpha R_o$$

where d' is the actual length of a lens element and α is a parameter whose magnitude depends on the relative dimensions of d' and R_o. In most cases a reasonable approximation is obtained with

$$\alpha \approx 1/4 \quad .$$

APPENDIX II

The Matrix Formulation of Geometrical Optics

The following sign convention will be adopted:
The object distance S_o is considered positive if the object lies in object space (ie. on the entrance side of the lens in the case of a thin lens);
The image distance S_i is considered positive if the image lies in image space;
A positive focal length f corresponds to a convergent lens.

The Thin Lens

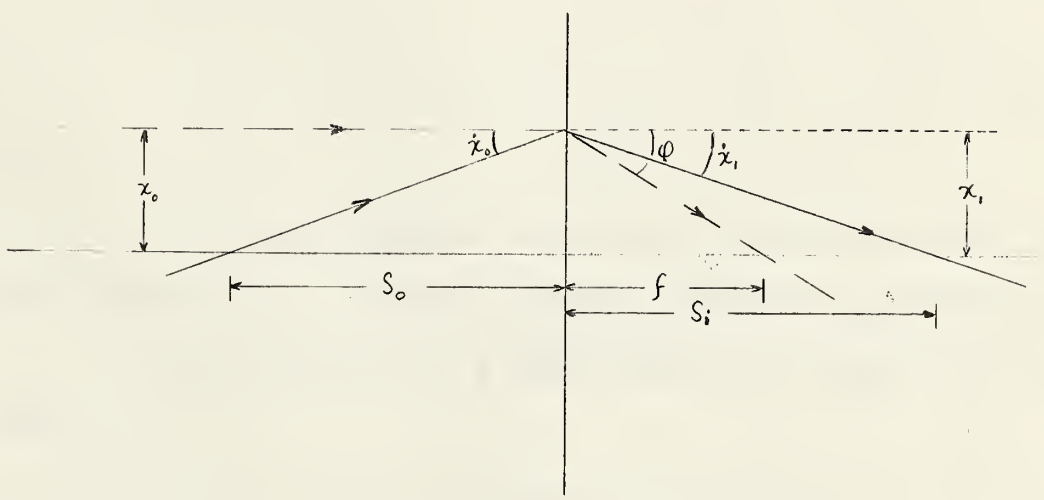

A ray incident parallel to the axis is bent through an angle φ where, from the diagram $\varphi \approx - x_1/f$.

A ray incident at angle $\dot{x}_o$ at distance x_o from the axis emerges from the lens at distance $x_1 = x_o$ from the axis and at an angle $\dot{x}_1$, where from the diagram,

$$\dot{x}_1 = \dot{x}_o - x_o/f$$

(which is the thin lens relation).

Thus if we wish to consider the properties of a thin lens in terms of a matrix transformation between object and image space,

$$\begin{pmatrix} x_1 \\ \dot{x}_1 \end{pmatrix} = M \begin{pmatrix} x_o \\ \dot{x}_o \end{pmatrix}$$

it is clear that the transformation matrix M must have the form:

$$M = \begin{pmatrix} 1 & 0 \\ -1/f & 1 \end{pmatrix} \qquad (1)$$

A transformation matrix may also be written for a drift space (ie. a region having no focussing properties).

By definition, a drift space of length L is such that:

$$x_1 = x_o + \dot{x}_o L$$

$$\dot{x}_1 = \dot{x}_o$$

and hence the matrix for a drift space is:

$$D = \begin{pmatrix} 1 & L \\ 0 & 1 \end{pmatrix} \qquad (2)$$

To illustrate the approach in using the matrix method consider the simple thin lens. A ray with coordinates in object space: x_o, $\dot{x}_o$, S_o is focussed in image space to a point with coordinates x_1, $\dot{x}_1$, S_i. Thus the ray "sees" a drift space of length S_o, a lens, and a drift space of length S_i, in that order. Hence the complete system is described by:

$$\begin{pmatrix} x_1 \\ \dot{x}_1 \end{pmatrix} = \begin{pmatrix} 1 & S_i \\ 0 & 1 \end{pmatrix} \begin{pmatrix} 1 & 0 \\ -1/f & 1 \end{pmatrix} \begin{pmatrix} 1 & S_o \\ 0 & 1 \end{pmatrix} \begin{pmatrix} x_o \\ \dot{x}_o \end{pmatrix}$$

or

$$\begin{pmatrix} x_1 \\ \dot{x}_1 \end{pmatrix} = \begin{pmatrix} 1 - S_i/f & S_i + S_o - \dfrac{S_o S_i}{f} \\ -1/f & 1 - S_o/f \end{pmatrix} \begin{pmatrix} x_o \\ \dot{x}_o \end{pmatrix}$$

Considering rays originating from a point on the axis and requiring point focussing, we have $x_1 = x_o = 0$ and hence:

$$\left(S_i + S_o - \frac{S_o S_i}{f}\right) \dot{x}_o \equiv 0$$

and since $\dot{x}_o \neq 0$

$\therefore$ $S_i + S_o - \dfrac{S_o S_i}{f} = 0$ which is the thin lens relation.

Thick Lenses or Combinations of Two Thin Lenses

In order to retain the simple thin lens relation in the case of the thick lens or a combination of two thin lenses, principal planes are introduced. Effectively, the thick lens (or lens combination) is replaced by an equivalent thin lens which is the principal plane. Two such planes are required, their location being such that when distances are measured relative to them, the simple thin lens relation is valid. The situation is illustrated in the following diagram.

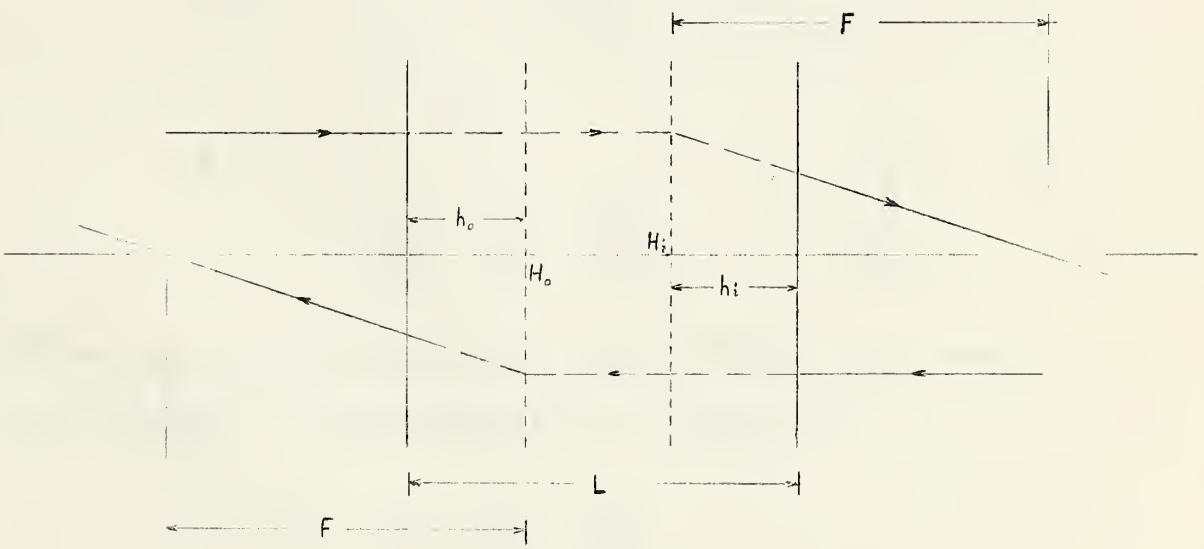

The following sign convention regarding the positions h_o and h_i of the object and image principal planes should be noted.

The object (entrance) principal plane is located

a distance h_o behind the lens entrance. The image (exit) principal plane is located a distance h_i before the lens exit.

An expression for the equivalent focal length of a combination of two thin lenses and expressions for the positions of the principal planes may be obtained easily using the matrix method.

Consider two thin lenses of focal lengths f_1 and f_2 separated a distance L. The transformation through the combined system of lenses and drift space is given by:

$$M = \begin{pmatrix} 1 & 0 \\ -1/f_2 & 1 \end{pmatrix} \begin{pmatrix} 1 & L \\ 0 & 1 \end{pmatrix} \begin{pmatrix} 1 & 0 \\ -1/f_1 & 1 \end{pmatrix}$$

$$M = \begin{pmatrix} 1 - L/f_1 & L \\ -\frac{1}{f_2} - \frac{1}{f_1} + \frac{L}{f_1 f_2} & 1 - \frac{L}{f_2} \end{pmatrix} . \qquad (3)$$

By comparison with the matrix for a single thin lens the focal length of the combination is given by:

$$\frac{1}{F} = \frac{1}{f_1} + \frac{1}{f_2} - \frac{L}{f_1 f_2}$$

To find the locations of the principal planes consider a ray incident parallel to the axis, from the object side of the system. Such a ray, by definition must cross the axis at distance F from the exit principal plane, ie. at distance $F-h_i$ from the lens exit. Thus, if we consider the

system of lens and drift space of length $F - h_i$, with conditions $\dot{x}_o = 0$, $x_1 = 0$, we must have:

$$\begin{pmatrix} 0 \\ \dot{x}_1 \end{pmatrix} = \begin{pmatrix} 1 & F - h_i \\ 0 & 1 \end{pmatrix} \begin{pmatrix} 1 - L/f_1 & L \\ -1/F & 1 - L/f_2 \end{pmatrix} \begin{pmatrix} x_o \\ 0 \end{pmatrix}$$

from which $0 = -L/f_1 + h_i/F$

and hence $h_i = LF/f_1$

Similarly, by considering rays parallel to the axis incident from the image side of the system, we find:

$$h_o = LF/f_2 \ .$$

Using the three relations just obtained, L may be eliminated from the matrix for the system. We find:

$$M = \begin{pmatrix} 1 - h_i/F & h_o + h_i - \dfrac{h_o h_i}{F} \\ -1/F & 1 - h_o/F \end{pmatrix} \qquad (4)$$

which, it may be verified, is equivalent to:

$$M = \begin{pmatrix} 1 & h_i \\ 1 & 1 \end{pmatrix} \begin{pmatrix} 1 & 0 \\ -1/F & 1 \end{pmatrix} \begin{pmatrix} 1 & h_o \\ 0 & 1 \end{pmatrix}$$

which is the transformation appropriate to a thick lens.

From equation (4) expressions may be obtained for the focal length and positions of the principal planes in terms of matrix elements for the lens. We find:

$$F = -1/M_{21}$$

$$h_i = \frac{M_{11} - 1}{M_{21}}$$

$$h_o = \frac{M_{22} - 1}{M_{21}}$$

These expressions, it will be realized, are of completely general validity, since any lens system can be reduced to an equivalent set of principal planes.

It is also of interest to note that the matrix for any lens system is orthogonal (ie. has determinant unity) as may be verified by inspection of equation (4).